Synthesis, Characterization and Antimicrobial activity of *Dioscorea alata* plant Extract Mediated Manganese Dioxide Nanoparticles

Mahbuba Kedir Abdo

A Thesis submitted to Department of Applied Chemistry

School of Applied Natural Science

In partial fulfilment of the requirements for the Degree of Master Science in Applied Chemistry (Industrial Chemistry)

Office of Postgraduate Studies

January, 2024
Adama, Ethiopia

Synthesis, Characterization and Antimicrobial activity of *Dioscorea alata* plant Extract Mediated Manganese Dioxide Nanoparticles

Mahbuba Kedir Abdo

Advisor: Prof. Tegene Desalegn

Thesis Submitted to the Department of Applied Chemistry

School of Applied Natural Science

In partial fulfillment of the requirements for the Degree of Master of Science in Applied Chemistry (Industrial Chemistry)

Office of Post Graduate Studies

Adama Science and Technology University

January, 2024

Adama, Ethiopia

APPROVAL OF BOARD OF EXAMINERS

We, the undersigned, members of the Board of Examiners of the final open defense by Mahbuba Kedir have read and evaluated her thesis entitled "Synthesis, Characterization and Antimicrobial Activity of *Dioscorea alata* Plant Leaf Extract Mediated Manganese Dioxide Nanoparticles'' and examined the candidate. This is, therefore, to certify that the thesis has been accepted in partial fulfillment of the requirement of the Degree of Master of Science in Applied Chemistry.

Advisor	Signature	Date
Chairperson	Signature	Date
Internal Examiner	Signature	Date
External Examiner	Signature	Date

DECLARATION

I hereby declare that this M.Sc. thesis titled **"Synthesis, Characterization and Antimicrobial Activity of *Dioscorea alata* Leaf Extract Mediated Manganese Dioxide Nanoparticles"** is my original work and has not been presented for a degree in any other university and all sources of material used for this thesis has been duly acknowledged through citation

Mahbuba Kedir	_____	_____
Name of student	Signature	Date

RECOMMENDATION OF ADVISOR/ SUPERVISORS

I, the advisor of this thesis, hereby certify that I have read the revised version of the thesis entitled **"Synthesis, Characterization and Antimicrobial Activity of *Dioscorea alata* Leaf Extract Mediated Manganese Dioxide Nanoparticles"** by Mahbuba Kedir submitted in partial fulfillment of the requirements for the degree of Masters of Science in Applied Chemistry (Industrial Chemistry). Therefore, I recommend the submission of a revised version of the thesis to the department following the applicable procedures.

_____	_____	_____
Advisor	Signature	Date

APPROVAL PAGE

I, the advisors of the thesis entitled **"Synthesis, Characterization and Antimicrobial Activity of *Dioscorea alata* Leaf extract Mediated Manganese Dioxide Nanoparticles"** and developed by Mahbuba Kedir hereby certify that the recommendation and suggestions made by the board of examiners are appropriately incorporated into the final version of the thesis.

_____	_____	_____
Advisor	Signature	Date

APPROVAL OF BOARD OF REVIEWERS

We, the undersigned, members of the Board of Examiners of the thesis by Mahbuba Kedir have read and evaluated the thesis entitled **"Synthesis, Characterization and Antimicrobial Activity of *Dioscorea alata* Leaf extract Mediated Manganese Dioxide Nanoparticles"** and examined the candidate during the open defense. This is, therefore, to certify that the thesis is accepted for partial fulfillment of the requirement of the degree of Master of Science in Applied Chemistry (Industrial Chemistry).

_____	_____	_____
Chairperson	Signature	Date
_____	_____	_____
Internal Examiner	Signature	Date
_____	_____	_____
External Examiner	Signature	Date

Final approval and acceptance of the thesis are contingent upon the submission of its final copy to the Office of Postgraduate Studies (OPGS) through the Department Graduate Council (DGC) and School Graduate Committee (SGC).

_____	_____	_____
Department Head	Signature	Date
_____	_____	_____
School Dean	Signature	Date
_____	_____	_____
Office of Postgraduate Studies, Dean	Signature	Date

ACKNOWLEDGEMENTS

First, I give all the glory and honor to Allah the source of all wisdom, knowledge, understanding, health, and strength. Then, I would like to express my honorable thanks to my family, particularly for giving me this chance to study at Adama Science and Technology University (ASTU). And foremost, the completion of this research work would not have been possible without the excellent guidance of my advisor, Prof. Tegene Desalegn. I acknowledge all his encouragement and valuable time given to me with deep gratitude and appreciation.

I would also like to acknowledge all the academic staff members and laboratory assistants of Department of Applied Chemistry at ASTU. Finally I must express my very profound gratitude to all my partners for providing me with unfailing support and continuous encouragement throughout my years of study and through the process of researching and writing this thesis. This accomplishment would not have been possible without them. Thank you all.

Contents **Page**

LIST OF FIGURES

LIST OF TABLES

LISTS OF ABBREVIATIONS AND ACRONYMS

C. Albicans	*Candida Albicans*
CFUs	Colony forming units
D.alata	*Dioscorea alata*
DMSO	Dimethylsulfoxide
E. coli	*Escherichia coli*
E. faecalis	*Enterococcus faecalis*
FT IR	Fourier Transforms Infrared spectroscopy
$KMnO_4$	Potassium permanganate
MHA	Mueller-Hinton agar
MnO_2	Manganese dioxide
MRI	Magnetic resonance imaging
NPs	Nanoparticles
P. aeruginosa	*Pseudomonas aeruginosa*
rpm	revolution per minute
S. aureus	*Staphylococcus aureus*
SEM	Scanning Electron Microscopy
UV- Vis	Ultraviolet Visible Spectrophotometer

ABSTRACT

In the field of nanotechnology, metal and metal oxide nanoparticles have attained a great significance due to their unique properties. Manganese dioxide nanoparticles have attracted high attention in recent studies due to its potential applications like antibacterial, antifungal and anti-cancer. In this study synthesis of Manganese dioxide nanoparticles was done using biological/green synthetic method from indigenous 'Dioscorea alata is a medicinal plant which commonly grows in south West Ethiopia. The synthesized MnO_2 nanoparticles were characterized using X-ray diffraction (XRD), Scanning Electron Microscope (SEM), UV-Visible and Fourier Transform Infrared spectroscopy (FTIR). The average crystal size of the synthesized NPs was calculated using the Debye Scherer equation. The average crystal size of MnO_2 NP was found to be 16.73nm (1:2 ratio), 9.60 nm (1:1), 16.90 nm (2:1) calcinated, and 7.13 nm (1:2) 5.72 nm(1:1) and 7.76 nm(2:1) uncalcinated MnO_2 NPs for green synthesis method. The XRD pattern with sharp peaks describes the crystalline and purity of Manganese dioxide nanoparticles. The FTIR spectrum of Manganese dioxide (Mn-O) nanoparticles absorbs at 557 cm^{-1} and 547 cm^{-1} for both calcined and uncalcinated respectively. Furthermore, the antibacterial and antifungal activity of the synthesized MnO_2 nanoparticles were evaluated against clinical and standard strains of Escherichia coli, Pseudomonas aeruginosa Staphylococcus aureus and Enterococcus faecalis by disc diffusion method using the suspension of bacteria spread on MH agar. The positive control for antibacterial testing was ciprofloxacin. According to this study, MnO_2 nanoparticles synthesized using Dioscorea alata leaf extract showed promising result against both gram-positive and gram-negative bacterial strains with maximum inhibition zone of 17.66nm E. faecalis and 16nm E.coli respectively. The positive control used for antifungal testing was Gentamycin.

Keywords: *Manganese dioxide nanoparticles, Green synthesis, Dioscorea alata, antimicrobials activity*

1. Introduction

1.1. Background of the study

Nanoscience and nanotechnology are significant scientific fields that deal with the use and development of materials made at the nanoscale. Nanotechnology involves synthesis, characterization and application of nanoparticles by controlling shape and size.

Nanoparticles (NPs) with sizes in the range of 1–100 nm can be produced through numerous methods. However, most of these methods use chemicals that have high risk of toxicity and low degradability (Ansar S, *et al*, 2020). Due to their small size and high surface-to-volume ratio, NPs have high effectiveness and durability, being employed in various fields, including biological, physical, chemical, pharmaceutical, and engineering sciences (Joshi NC *et al, 2020).*

In the field of nanotechnology, metal and metal oxide nanoparticles have attained a great importance due to their unique optical, catalytic, electronic, magnetic and antimicrobial properties owing to their small size (Okuda *et al*. 2005). Nanomaterials have attracted extensive attention owing not only to their fundamental significance, but also to the potential technological applications in various fields. Materials at the nano level have improved magnetic, electric and catalytic properties than that of bulk materials. So, nanomaterials can be utilized in various fields of medicine, electrical devices, environment etc.

The synthesis of nanoparticles is critical to understand the particulate formation process, modify the physicochemical properties of the nanoparticles and enable specific functionalities and application.

Nanoparticles can be manufactured by simple techniques and in addition, it uses cost-effective wet chemical techniques such as hydrothermal, sol-gel, emulsion, conventional precipitation, and it has a broad range of applications in the industrial sector (Cherian E, *et al*, 2016). Recently biological methods of synthesis of nanoparticles using enzymes of microorganisms and plant extracts have been suggested as possible eco-friendly alternatives to chemical and physical methods (Awwad *et al*., 2014). Green synthesis of nanoparticles and

their application in food processing, production of antimicrobials, cosmetics and healthcare products have been acknowledged by number of researchers (Awwad *et al*., 2014).

Manganese dioxide nanoparticles, MnO_2 NPs a promising material has attracted considerable interests in virtue of its low cost, high environmental compatibility and wide structural diversity combined with unique physical and chemical properties (Easton DF *et al*, 2015 and Morales L,*et al*, 2013). Transition-metal oxides have been shown to be excellent electrode active materials due to their chemical stability, variable valence etc.

The main applications of nano-sized MnO_2 NPs include preparation of cathode materials of alkaline batteries (Cao HX *et al*.2011), electrochemical capacitors (Diego EJ *et al*, 2016), smart windows (Ferrero JM *et al*,2017), the active layer for gas sensors (Burstein HJ, et al, 2014), photocatalyst (Draganescu M *et al*, 2017), day removal, adsorbents and catalytic materials (Robinson D. M., Go Y. B., Mui M., *et. al*., 2013; Shaban M., Abukhadra M. R., *et.al*, 2017).

Synthesis of nanoparticles using plant extract is one of the biological/green synthesis methods used because of their environment friendly, cost effectiveness, and uses safe reagents during the production of nanoparticles.

Dioscorea alata commonly known as ‘’greater yam‟ and locally known as ‘godere’ are climbing perennial vines with heart-shaped leaves (Figure 1). Being rich in starch content and well known for their edible tubers, the plant serves as important staple foods and potential sources of ingredients for fabricated foods in Southwest Ethiopia (Das *et al*, 2012; Huang *et al*, 2006). Among various yams, Dioscorea alata is also known for its high nutritional value, with a crude protein, vitamin C(Osagie *et al*, 1992), minerals and carbohydrate(Kochhar *et al*, 1981).

There exist reports of researches done on various medicinal and clinical aspects of the *Dioscorea alata* tubers (Das *et al*., 2012; Chen *et al*., 2003), but there is not much work done on leaf part of the plant for biomedical activity.

Figure 1: *Photo of* Dioscorea alata *used for synthesis of MnO_2 NPs.*

The previous work deals with the phytochemical analysis and a comparative assessment of possible antioxidant, and anticancer activities of the 70% methanolic and aqueous extracts of *Dioscorea alata* leaves followed by the analysis of the availability and abundance of different phytochemicals (Abhishek Das *et al* 2014).

In this research, MnO_2 NPs were synthesized using leaf extract of *Dioscorea alata* for evaluation of its antibacterial activity against selected gram-positive and gram-negative bacterial strains and antifungal activity.

1.2. Statement of the Problem

The use of *Dioscorea alata* plant leaf extract in the green production of Manganese dioxide nanoparticles (MnO_2NPs) and their application for antimicrobial is motivated by a few fundamental issues.

The first is the daily rise in microbial infectious diseases and the rise in bacterial and fungal resistance to previously used antimicrobials; as a result, it is getting harder for communities

to choose an effective antimicrobial drug empirically. Bacterial infection diseases are a severe public health issue that has gained international attention as a hazard to human health that also has implications for the economy and society.

It is crucial to teach society about the medical benefits of this natural resource because humans rely heavily on nearby natural resources to maintain their health different types of bacteria, fungi, and even plants are used to make various antibacterial and antifungal medications.

However, some antibiotics are extremely expensive, and others are hazardous to both people and the environment. To ensure our society's survival and health against numerous diseases, it is necessary to discover the simplest ways for synthesizing affordable and nontoxic medications.

In this study, MnO_2 NPs has been synthesised using leaf extract of *Dioscorea alata* plant. Since it uses locally accessible resources, green synthesis is environmentally safe, non-toxic, and cost-effective. No research work has reported at this plant in terms of synthesizing MnO_2NPs for antimicrobial activity tests using the leaf extract as a capping and reducing agent. Therefore, this work was intended to explore the potential of the green synthesis route to induce further investigations in these areas using *Dioscorea alata* leaf extract.

1.3. Objectives of the Study

1.3.1. General objective

The general objective of this study is to synthesize MnO_2 nanoparticles using *Dioscorea alata* plant leaf extract and evaluate its antimicrobial activity.

1.3.2. Specific objectives

- To synthesize MnO_2 nanoparticles using leaf extract of *D.Alata* and potassium permanganate ($KMnO_4$) salt as precursor.
- To characterize the synthesized MnO_2nanoparticles using UV-Vis, XRD, FTIR and SEM spectroscopic techniques.
- To study the antibacterial and antifungal activities of MnO_2 nanoparticles against two gram-positive and two gram-negative bacterial pathogens and one fungal strain.

1.4. Significance of the Study

The result of this study could serve as baseline information for the researchers for further study. It also provides data on the potential use of a low cost, simple, and environmentally eco-friendly green synthetic routes using *D. alata* leaf extract to produce MnO_2 NPs.

The result also shows the application of D.alata for NPs synthesis in addition to its usual use as food and traditional medicine.

1.5. Scope of the Study

The scope of this study was limited to the synthesis of MnO_2 NPs using *Dioscorea alata* leaf extract, characterizations of the synthesized nanoparticles using, UV-Vis, XRD, FT-IR, and SEM, and the evaluation of the antimicrobial activity of the synthesized MnO_2 nanoparticles against selected bacterial and fungal strains.

2. Literature Review

2.1. Introduction to Nanomaterials and Nanoparticles

Nanoparticles (NPs) are the fundamental component of nanotechnology. Nanoparticles are the particulate matters with at least one dimension less than 100 nm. The nanoparticles (NPs) can exist in different shape, size and structure such as spherical, cylindrical, tubular, conical, hollow core, spiral, flat, wire etc. The physio-chemical properties of these NPs are mostly influenced by their variation in size & shapes. Nanoparticles are synthesized by both chemical and physical means for a long time, but the use of biological systems and microorganisms in the production of metal nanoparticles is under rapid growth in recent time owing to its greener route and ease of formation of nanoparticles. Recently there has been found much interest in the synthesis of nanoparticles by green means owing to their considerably improved properties over bulk metal (Annu, Akbar Ali, and Shakeel Ahmed *et al*, 2018). Owing to unique physical and chemical properties, NPs has achieved great success in wide variety of applications in different fields such as medicinal, environmental, energy-based research, imaging, chemical & biological sensing, gas sensing etc. Researchers are more inclined towards nanotechnology as it is considered as one of the important factors for a clean and sustainable future (Kumari and Leena Sarkar *et al*, 2021). Nanomaterials have been extensively discovered with unique properties and brilliant capabilities since they pave the way for developing multidisciplinary researches, and applying for solving many practical problems. Indeed, they have brought many advantages and desirable prospects for human life such as medicine, pharmaceuticals, agriculture, environment, catalysis, food, cosmetics, and electronics (Ghotekar *et al*. 2020). The main reason may rely on their tiny size, diverse structure, and many biochemical and physicochemical properties, which are suitable for many different fields. Nanomaterials have appeared as novel antimicrobial agents containing a high-surface area to volume ratio and the inivitable photochemical properties (Jalal R., Goharshadi E.K., Abareshi M. *et al*, 2010).

Nanomaterials are also being employed in the medical profession for remedial drug discovery and delivery for many sicknesses (A.Y Hoseinpour V., Ghaee A., Vatanpour V *et.al*, 2018). Most current NPs and NMs can be organized into four material-based categories such as Carbon-based nanomaterials, Inorganic-based nanomaterials, Organic-based nanomaterials

and composite-based nanomaterials. Nanomaterials classified based on their dimensions such as 0D, 1D, 2D and 3D NMs (Ahmed Barhoum *et al*, 2018).

Metallic/metal oxide nanoparticles are considered to be the most superior, possibly thanks to their large surface area to volume ratio, high biocompatibility, tuneable synthesis, and high stability (Ahmed *et al*, 2016).This leads to the huge interest of researchers in the development and synthesis of nanoparticles.

Metal oxide nanoparticles (NPs), due to their excellent surface area to volume ratio, surface energy, spatial confinement and reduced imperfections, have characteristics of physico chemical, electrical, mechanical, magnetic, thermal, dielectric, optical and biological confidants as compared with other materials (G. A., Tobaldi D.M., Ansell M.P., *et.al*,2016 ; Deng A., Zhu Y., Zhou L.,*et.al*,2018).

Manganese oxide nanoparticles have engrossed consideration due to their extensive applications in several fields such as catalysis, ion-sieves, rechargeable batteries, chemical sensing devices, Microelectronics (Dang T.-D. *et.al*, 2013) and optoelectronics (Prasad K.S., Patra A.*et.al*, 2017). Furthermore, due to the existence of numerous attachments for a diversity of usage, they are based against earth extra elements, as Mn is the twelfth most plenty element on the planet and the third most common transition element after Fe and Ti (Veeramani H., Aruguete D *et.al*, 2013). Moreover, the manganese dioxide nanoparticles (MnO_2NPs) have a good photocatalytic activity for dye degradation (Souri M., Hoseinpour V *et.al*, 2018 and -Fei J.B., Cui Y., Yan X.H. *et.al*, 2008).

2.2. Metal Nanoparticles

Metal NPs have a high specific surface area and a high fraction of Metal nanoparticles surface atoms; have been studied extensively because of their unique physicochemical characteristics including catalytic, optical, electronic, mechanical, thermal, dielectric magnetic properties and antimicrobial activities (Krolikowska *et al*, 2003; Zhao and Stevens *et al*, 1998). Most of the current strategies are usually working by the use of physical or chemical principles to synthesize metal nanoparticles.

Metallic nanoparticle is nano sized metals with the size range of 10-100nm. Metal nanoparticles are submicron scale entities made of pure metals such as Ag, Au, Ti, Cu, Mn, Co, Zn and Mg.

In the medieval era, metallic nanoparticles were actually used to decorate cathedral windows. In various industrial applications, metallic nanoparticles have attracted attentions, because of their different physical and chemical properties from bulk metals. Catalysts which are used in metallic nanoparticles are selective and highly active, has long lifetime for many chemical reactions (Harish Kumar K *et al*, 2018).

Metal nanoparticles can be synthesized through green method plant extracts. According to reports (Harish Kumar K *et al*, 2018) different parts of the plants such as leaves, flowers, fruits, roots and peals etc have been used for synthesis of metal nanoparticles**.**

2.3. Metal Oxide Nanoparticles

Metal oxides play a very significant role in the science of materials, such as the production of microelectronic circuits, sensors, electronics, ceramics, pharmaceuticals, piezoelectric devices, fuel cells, surface passivation coatings and photo catalysts. Metal oxides have also been used as absorbers of the environmental pollutant.

In nanotechnology, oxide nanoparticles can show signs of unique chemical properties due to their limited size and high density of edges.

The common metal oxide NPs are copper oxide, calcium oxide, magnesium oxide, zinc oxide, titanium dioxide, cobalt oxide, manganese oxide, and iron oxides (B.Ramola and N.C. Joshi, Y. Prakash *et al*, 2019). The MnO_2 NPs also have many applications in different fields of science and technology. TiO_2 NPs are among the most widely produced metal oxide NPs which is mainly due to its respectable and versatile properties originating from the physical, chemical stability, optical, and electrical. Anatase, brookite, and rutile are its different mineral forms, but generally, TiO_2 exists in the former one due to enhanced photocatalytic activity. Despite the importance of TiO_2 NPs, very few attempts have been made for its green production.

Green synthesized ZnO NPs are other most beneficial metal oxide nanoparticles due to their rapid rate of formation, nontoxicity significant biocompatibility, antimicrobial activity, and photocatalytic activity. The plant extract is used as a biological reducing and stabilizing agent in the synthesis of ZnO NPs. Fungi and other microorganisms have also been used to prepare ZnO NPs. ZnO NPs are considered to be the most significant nanoparticle mainly due to their increased surface area-to-volume ratio and have been utilized in various science and engineering fields such as electrochemistry, catalysis, medical devices, cleaning agents, textile industry, etc.

Fe_2O_3 NPs are another explored transition metal oxide NPs because of its impact on the development of materials utilized in the field of magnetism, catalytic, sensor, optics, and biomedical, due to their characteristic electrical, magnetic, optical, and electronic, and catalytic properties. It generally exists in different minerals such as hematite (α-Fe_2O_3), bixbyite (β-Fe_2O_3), maghemite (γ-Fe_2O_3), ε-Fe_2O_3, magnetite (Fe_3O_4), and w*ü*stite (Fe-O). Out of these, hematite is thermodynamically the most stable one due to its small size and large surface area. Furthermore, hematite is cost effective, abundant, nontoxic, and biocompatible and hence applied in biomedical field (Narayanan KB *et al,* 2016).

CoO NPs have good catalytic activity property with cost efficiency. Hence, CoO NPs can be used in manufacturing sensor and biosensor and as catalyst. Due to high surface to volume ratio, size controllability and high stability CoO NPs have been exploited in various applications.

In addition to the above mentioned metal oxide nanoparticles, MnO_2 NPs are one of the best nanoparticles used in sensors, energy storage, catalysis, environmental remediation, and antimicrobial activities (Joshi N.C., Joshi E. *et al*, 2020; Hoseinpour V., Souri M. *et al*, 2018).

2.4. Manganese oxide Nanoparticles

Manganese oxide is one in all the foremost interesting materials, incorporates a large choice structure with large surface extent. MnO_2 can exist in different structural forms α, β, γ, δ, ε, and λ types and so forth, when the basic structural unit ((MnO_6) octahedron) is linked in

different ways. Based on the different (MnO_6) links, MnO_2 can be divided into three categories: the chain like structure, the sheet or layered structure and the 3D structure (Y.Chen *et al*, 2002). The varied structures, chemical properties of manganese oxides are taken advantages of potential application like as cat ion-exchange, ion and molecules separation, absorbents, sensor, battery and catalysis etc.

Manganese oxide can be found in various valence states including, MnO (Mn^{+2}), Mn_3O_4 ($Mn^{+2.67}$), Mn_2O_3 (Mn^{+3}), and MnO_2 (Mn^{+4})(X. Cai and Q. Zhu *et.al* 2019). The valence state specifies the field of application. For instance, MnO_2 is used as an electrode in lithium-ion batteries and as a catalytic material in oxidation–reduction reactions.

The presence of Mn^{+3} ions in the MnO_2 lattice as MnO-OH leads to the transfer of electrons between Mn^{+4} and Mn^{+3} ions. Such a mechanism is responsible for the catalytic activity in nonstoichiometric manganese oxide. Mn_2O_3 proved its importance to the manufacture of soft magnetic materials, and it is also used as a catalyst for the removal of carbon monoxide from waste gas and Mn_3O_4 ($Mn^{+2.67}$), has attractive electro chromic properties such as the change of its optical transmittance in the visible spectrum with an applied voltage which makes it candidate or window applications. MnO_2 is considered as one of the best catalysts due to its low cost and less toxicity, environmental compatibility (W.Li, *et al*, 2012 and L.X.Zhang *et al*, 2014).

Among many transition metal oxides, Manganese oxide exhibit different forms of which MnO_2 is the one of the most attractive oxide due to its unique properties. Manganese (iv) dioxide (MnO_2) NPs has a low band gap, high optical constant semiconductor that exhibits ferroelectric and catalytic properties (Shao-Horn Y *et al*, 1998 and Zoltowski P *et al*.,1993). The bandgap (Eg) of MnO_2 (β-MnO_2: 1.0 eV, α-MnO_2: 1.2 eV) is smaller as compared to other inorganic UV absorbers. The bandgap of MnO_2 NPs can also be varied depending on their morphologies and crystal structures (δ-MnO_2 nano sheet: ~ 3.8 eV,α-MnO_2 nanowire: ~ 3.3 eV, α-MnO_2 nano rod ~ 2.8 eV).

MnO_2 NPs can be synthesized by many different chemical and physical methods, such as atomic layer deposition(A. Vijayamari, K. Saday *et.al*,2017; Sun A. Moon *et.al*,2015) , liquid-phase electrochemical method, pulsed laser deposition, chemical bath deposition,

electron beam deposition, thermal evaporation ,hydrothermal, sol–gel, and chemical spray pyrolysis(A. Vijayamari, K. Saday *et.al*,2017; SunA.Moon *et.al*,2015; S.C. Vella Durai1 E. Kumar *et.al*,2020). However, these kinds of methods usually use organic solvents and toxic reducing agents, the majority of which are highly reactive and harmful to the environment. Therefore, to minimize the impact on the environment, recent reports indicate that green synthesis processes have become procedures of choice to synthesise metal oxid nanoparticles.

2.5 Properties of MnO_2 nanoparticle

2.5.1 Crystallinity

The dimension of manganese oxides at the nanoscale impacts the properties mainly in two aspects: (i) a change in structural features (viz., the lattice symmetry and cell parameters) and (ii) the presence of low coordinated atoms (viz., corners or edges or oxygen vacancies).

The structural properties of manganese oxides that adopt versatile geometries in different oxidation states are quite fascinating. Tetravalent oxide, MnO_2 is crystallized as single phase stable tetragonal structure and can incorporate various actions as well as water molecules inside the "tunnels" or "channels" between the [MnO_6] octahedral (Feng, Q.; Kanoh et al, 1999, Shen *et al*, 1993 and Suib *et al* 2008). The family of MnO_2 with specific crystallographic faces and unique morphologies largely determine their functional properties.

Among the manganese dioxides, α-MnO_2 stabilizes in body-centred tetragonal lattice, while, β-MnO_2 crystallizes as the pure tetragonal/rutile structure (Chen, Z.; Jiao *et al,* 2012 and Djerdj *et al*, 2007) γ-MnO_2 is poorly crystalline as it is the product of intergrowth of the elements of pyrolusite and ramsdellite and as a result, complete single crystal does not emerge in this structure.

2.5.2. Magnetic properties

The family of manganese oxides provides an eminent platform to alter the intrinsic magnetic ordering by manipulation of size, shape and internal strain of the colloidal particles.
Magnetic properties of manganese oxide nanostructures have attracted considerable interest during the past three decades as manganese is expected to adopt different local configurations, including room-temperature ferromagnetism that is hard to achieve. The

magnetic properties of these oxides with dimension at the nanometre regime are of significance in diverse arenas of technological applications in high-density magnetic storage media, which have extensive applications in audio and video devices, electrical energy storage, electronics and information technologies, super capacitors, computer data storage, and as precursors for synthesizing soft magnetic materials(Ahmad *et al*, 2004). Magnetism of these oxides are also envisaged because of their promising applications in magnetic resonance imaging, Ferro fluid technology, spin valves, magneto caloric refrigeration, catalysis, and so on. Magnetic studies of MnO_2 nanostructures have shown an anti-ferromagnetic character with a ferromagnetic component.

The magnetic properties of the several structural forms (α-, β-, γ- and δ-) of MnO_2 elucidate numerous interesting features. The magnetization studies of α-MnO_2 explicate a characteristic spin glass behaviour below 50 K which is quite different from the bulk α-MnO_2. The local magnetic moment is enhanced in smaller dimensions because of the reduction in the number of neighbouring atoms compared to their bulk counterparts(S. K. Ghosh *et al*, 2020).

2.5.3 Semiconducting Properties

When the size of the materials shrinks into the nanoscale dimension, the occupied electronic states located above the valence band of the corresponding bulk materials augments the physical and chemical activities of the systems (De Abreu *et al*, 2018 and Schnedermann *et al*, 2018). It has been noted that the bandgap increases with decrease in size of the nanostructures. This is because as a result of the spatial confinement of the electrons in the conduction band and holes in the valence band, the lowest energy corresponding to the optical transition from the valence to conduction band increases, resulting in an increase of the effective bandgap of the semiconductors. MnO_2 is a n-type semiconductor with the energy band gap value as 3.26 eV. Pure α-MnO_2 behaves as a semiconductor with an indirect band gap of 1.3 eV, while β-MnO_2 has an energy band gap of 1.5 eV.

2.5.4. Optical properties

The α-MnO_2 NPs have high absorption in UV region with maximum absorption peak at 478 nm and moderately absorption in the Vis region. The absorption band around 478 nm is corresponding to energy of 2.60 eV. This band gap energy is blue shifted from bulk value of

2.1 eV which indicates the quantum confinement effect in α-MnO_2 NPs (N. Rajamanickam *et al*, 2014). The Eg value is close to the value 2.5 eV reported by Toufiq et al. for MnO_2 NPs synthesized by hydrothermal method (A.M. Toufiq *et al*, 2014) and the value 2.54 eV reported by Gagrani *et al*. for MnO_2 nano rods prepared by mechanic chemical processing (A. Gagrani *et al*, 2018).

In general, the optical band gap of materials is affected by disorders at the grain boundaries, defects, charged impurities, residual strain and confinement of the particle size (S.H. Mohamed, *et al*, 2010 and, P. Prathap *et al*, 2008). The compressive strain can lead to an increase in the band gap whereas the tensile strain can lead to a decrease of band gap. Thus, the obtained high Eg value may ascribe to the quantum confinement effects and the possible strains arise during preparation. High ultraviolet intense peak confirms the purity and the good crystallinity of the prepared samples in consistent with XRD results. On other side, the broad and less intense emission peak is due to a combination of several factors, amongst them: the transition of electrons from the shallow donors' levels of oxygen vacancies or Mn interstitial to the valence band, surface defects, dangling bonds and oxygen interstitial (A.M. Toufiq et al, 2014).

2.6. Synthesis Methods of Nanoparticles

In general, the methods for the synthesis of nanoparticles can be categorized into top-down and bottom-up (Figure 2). The top–down (breakdown) approach involves grinding down of large macroscopic particle into smaller particles. It involves synthesizing large-scale patterns initially and then reducing it into nanoscale level. The main disadvantage of the top-down approach is the imperfection of the surface structure. The second is the bottom-up (build-up) method that produces nanoparticles starting from atoms of gas or liquids based on atomic transformations or molecular condensations.

In the bottom-up approach, atoms and molecules are used as the building blocks in synthesizing complex nanostructures. Due to the high preparation cost and structural defects on produced NPs, the top-down approach is not widely used (Nikam A V *et al*, 2018). The bottom-up approach is preferred by most of the researchers as particles of uniform size and morphology can be obtained (Sonika Dawadi *et al*, 2020). Both approaches are used in the synthesis of metal oxide nanoparticles and relevant for determining the size, shape, and

properties of nanoparticles for specific application. The synthesis approaches are also classified into physical, chemical and biological synthesis depending on the processes or materials involved in the production process.

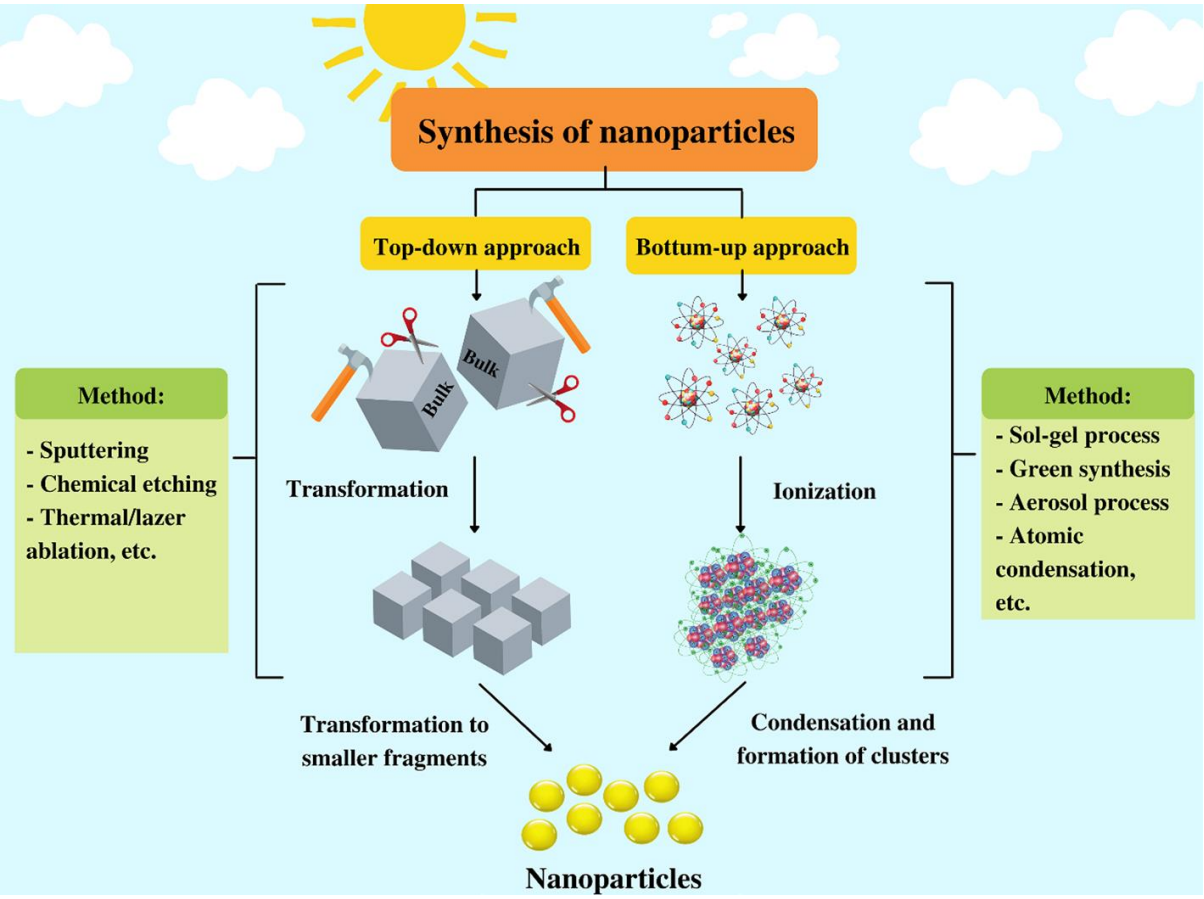

Figure 2: Different Synthesis Methods of Nanoparticles (Ngoan T. T. N. *et al*.2022).

2.6.1. Physical Method of Nanoparticles Synthesis

To synthesize nanoparticles, there are some widely used physical methods such as high-energy ball milling, electro spraying, laser ablation, physical vapour deposition, melt mixing, inert gas condensation, laser pyrolysis, and flash spray pyrolysis (Dhand *et al*, 2015; Vishnukumar *et a*l, 2017). These methods mostly belong to the top down approach by using mechanical energy or electrical energy to grind materials into small-size nano particles (Dhand *et al*, 2015).

Two of the most noteworthy methods are evaporation and condensation, carried out in a tube furnace to produce metallic nanoparticles at atmospheric pressure (Abbasi *et al*, 2014).

Although the physical methods are eco-friendly because they do not use toxic chemical substances, the grinding of materials is considerably energy-consuming and requires elaborate equipment, leading to high production cost, and difficulty of systematically scalability (Iravani *et al,* 2014).

2.6.2. Chemical Method

Chemical methods are extremely Moderate reaction conditions and convenient synthetic manipulation has made it an attractive option for accessing MnO_2 nanoparticles.

The method also provides better control of chemical and morphological characteristics There are different chemical methods such as: Micro-emulsion, chemical reduction, precipitation, hydrothermal techniques, Co-precipitation, sol-gel, solid-state synthesis, electrochemical and photochemical reduction techniques are most widely used for nanoscale synthesis (A.M. Abdelgawad and V. Hoseinpour *et al*, 2017). Chemical methods are extremely expensive and also involve the use of toxic, hazardous chemicals, which may pose potential environmental and biological risks.

2.6.3. Green Synthesis Method

Green synthesis is routes are good competent over the physical and chemical techniques. Green Chemistry principle based synthesis of nanoparticles have emerged as alternative to overcome the limitation of conventional methods (Salam *et al*., 2012; Sharma *et al*., 2009). Green synthesis mainly concerns the elimination of hazardous wastes and the utilization of sustainable processes, implementation of environmental friendly chemicals, solvents and renewable materials (Anastas and Warner *et al,* 1998; Matlack *et al,* 2001).

In the green-nanotechnology (Figure 3), various metal oxides nanoparticle synthesis have been reported using yeast, fungi, bacteria, algae, plant extract etc. From environmental point of view, plant extracts based reduction methods can be considered as more effective green approaches for synthesizing metal nanoparticles, because of employing plants towards synthesis of nanoparticles are emerging as advantageous compared to microbes with the presence of broad variability of bio-molecules in plants can act as capping and reducing agents (Duran *et al*, 2005; Duran *et al*, 2011; Narayanan *et al*, 2010).

Thus increases the rate of reduction and stabilization of nanoparticles and synthesis can be performed under mild experimental conditions such as relatively low reaction temperature and ambient pressure (Carmona *et al*, 2010).

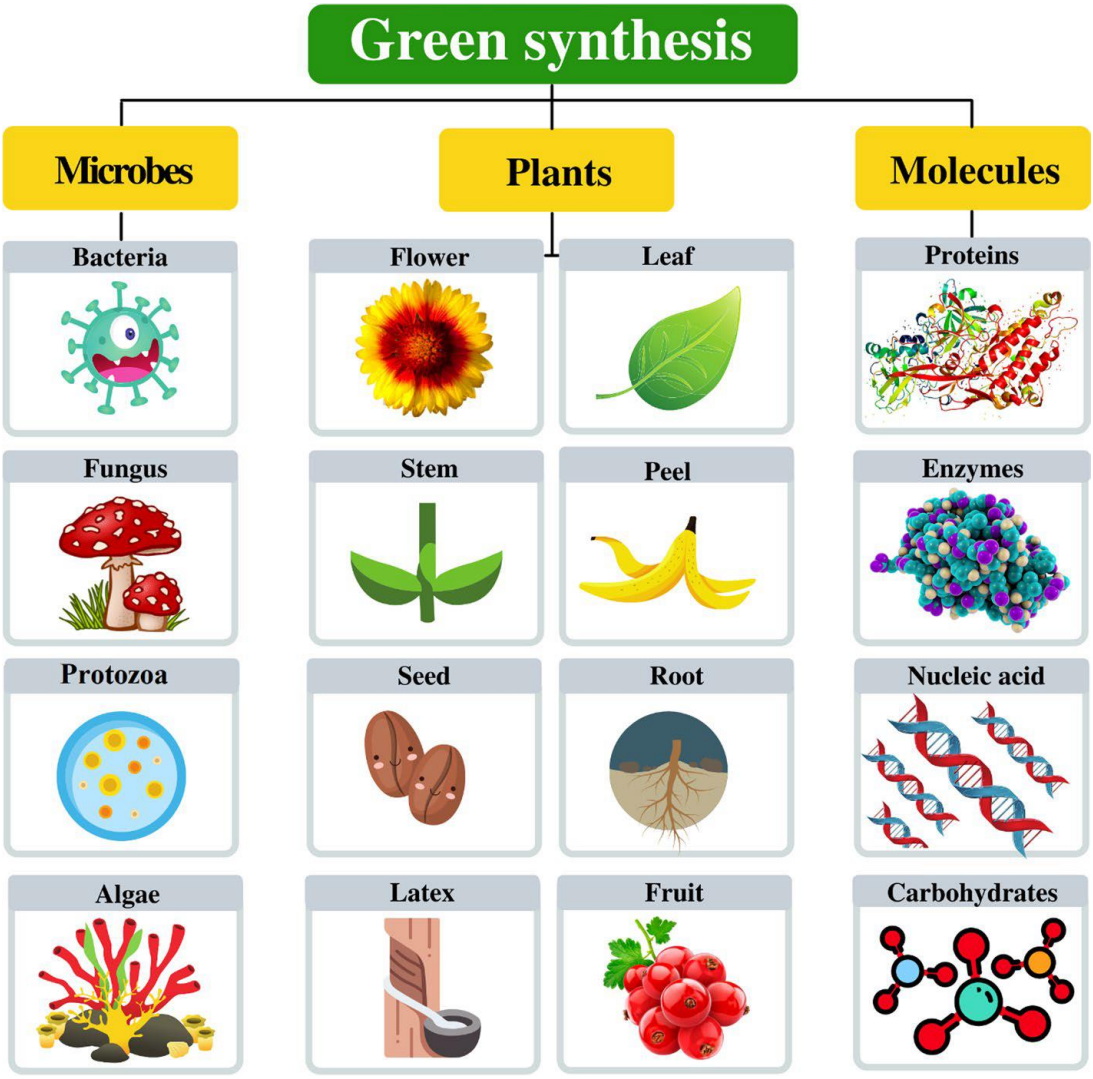

Figure 3: Green synthesis methods for synthesis of nanoparticles (*Ngoan Thi Thao Nguyen et al*.2022).

2.7. Characterization Techniques

Characterization of the synthesized sample is important in order to evaluate the success of the synthesis of the nanoparticles properties (Sanchez-Botero L *et.al*, 2017). Characterization of nanoparticles could be performed using a variety of analytical techniques (Figure 4), including UV-Vis spectroscopy, Powder X-ray Diffraction (XRD), Fourier transform infrared spectroscopy (FTIR) and scanning electron microscopy (SEM). The optical properties of the

nanoparticles can be determined by using UV- Visible spectroscopy (UV-Vis) in the wavelength range 200-800nm. The bandgaps of nanoparticles can be calculated from the UV-Vis absorbance/diffuse reflectance spectroscopic technique. The functional group of the nanoparticles is determined by Fourier Transform-Infrared Spectroscopy (FT-IR) in wavelength range 400-4000cm^{-1}.The morphology of nanoparticles is investigated with scanning electron microscope (SEM). Phase composition and purity of the nanoparticles is observed by X-ray diffraction (XRD).

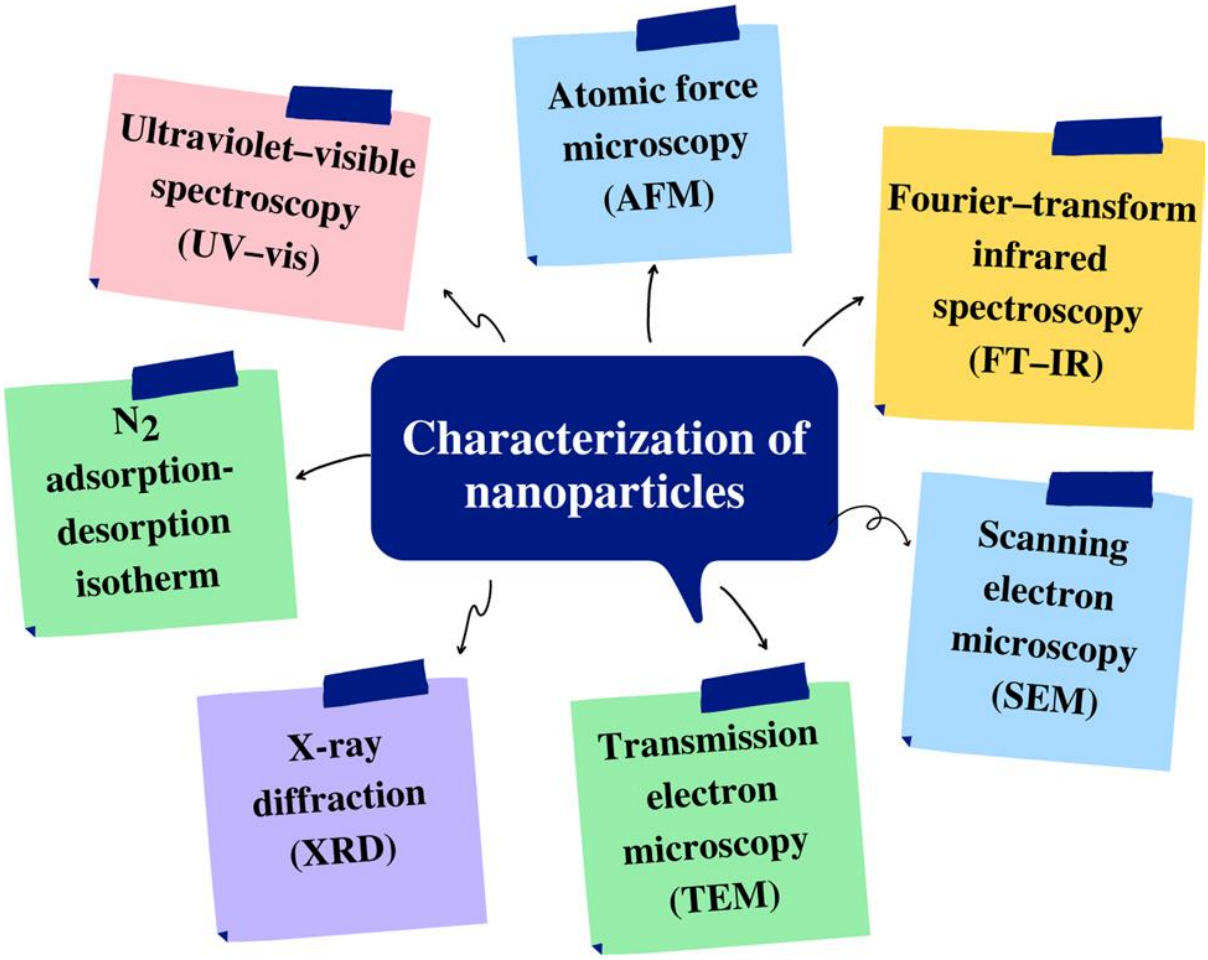

Figure 4: Different Characterization techniques for nanomaterials (Ngoan T.T. N. *et al*.2022).

2.8. Applications of Nanoparticles

Metal oxide nanoparticles can be applied in multiple functionalities. Because of their, excellent catalytic, optical, magnetic and electrochemical properties; metal oxide

nanoparticles can be used in energy conversion and storage, photocatalytic role, biomedical application and for environmental cleaning.

Manganese oxides have great potential toward a wide range of technological applications, such as, ores of metallic manganese, components in ferrite production, selective heterogeneous catalysts, cross-linking agent in rubber, sorbents, corrosion-inhibiting pigments, pollutant monitoring, chemical and biological sensors, and black innards for dry cell batteries (Rahaman, H.; Laha, R. M *et al*, 2015). manganese oxide materials have also been utilized in designing chemically powered artificial micro motors capable of interconverting chemical energy into mechanical energy that can be exploited for cargo delivery, detoxification, or motion-based sensing. The spinel structure has attracted great interest because of its potential technological applications, such as catalysis, ion exchange, molecular adsorption, and water treatment. (Chen, Z.*et al*, 2012) manganese dioxide (MnO_2) (pyrolusite) can be found in the Earth's crust as coatings, in massive deposits, and as important deep-sea minerals. (Sai Gautam *et al*, 2018).

Due to the chemical and physical properties, MnO_2 NPs has many applications. Manganese dioxides act as cathode materials for secondary batteries, and due to their catalysis and ion exchange reaction nature, they are used in magnetic resonance imaging (MRI).

Nanosize particles and crystal morphology play many important roles in these applications, which have driven researchers to focus on the MnO_2 nanoparticles in recent years. Out of many applications, antimicrobial, antioxidant and photocatalytic properties are the major ones. Catalytic activity of manganese and a relatively large surface area of nanoparticles (compared to bulk form) make manganese oxide nanoparticles a good candidate as a soil remediation agent.

Effective decontamination was reported, e.g., for arsenic, selenium, thallium, cadmium, and lead species in the soil MnO_2 NPs was proven to remediate soil and water contaminated with toxic dyes, released as industrial waste. MnO_2 NPs based biosensors can detect, i.e., glucosidase, glucose, or glutathione (GSH) in human blood or Salmonella typhimurium, a pathogenic bacterium, in food products.

Nanoparticles, which possess unique physicochemical properties, slowly enter the field of medical applications. The emerging tools and solutions develop into new branches, e.g., nano medicine or nanotheranostics. Nanomaterials have the potential to replace current techniques due to better biocompatibility, cell targeting ability, effective internalisation, etc (Zuzanna Sobanska, Joanna Roszak, *et.al*,2021).

2.8.1. Antimicrobial activity

The metal and metal oxide nanoparticles have gained a great attention due to their antimicrobial properties. Manganese dioxide (MnO_2) nanoparticles are one of them; due to nano sized particle sizes and some unique characteristics, such nanoparticles can easily enter in the cells of micro-organisms. After that, a significant inhibition mechanism takes place inside the microbial cells. This mechanism causes distortions and destroys cell membranes; finally, it resulting death of microbial cells (N. C. Joshil *et al*, 2020).

2.8.1.1. Antibacterial activity

Antibacterial activity may be affected by several factors, including mean particle size and shape, specific surface area, and surface curvature. The use of NPs in the fight against bacteria has led to a reduction in the frequency of bacterial infections (Dey N, *et al*, 2022). It was discovered that the inhibitory zone of manganese dioxide nanoparticles against Gram-positive bacteria, such as *S. aureus, S.coccus* and *Bacillus*, were much larger than Gram-negative bacteria. When tested against Gram-negative bacteria, manganese dioxide nanoparticles were more effective at inhibiting *K. pneumonia* than at inhibiting *Pseudomonas aeruginosa* (Cherian E, *et al*, 2016).

Through the disc diffusion method, it was established that some strains of *S. aureus* and *P. aeruginosa* are susceptible to MnO_2 nanoparticles when they are present in low quantities.
MnO_2 nanoparticles have been found to have a potential application in the battle against multidrug-resistant bacteria and other pathogens (Kunkalekar RK *et al*, 2013). It has been shown that the antibacterial activity of plant extract-stabilized manganese nanoparticles is more remarkable than that of plant extract alone against every bacterium. It is advocated that indigenous medicinal plants be utilized to synthesize nanoparticles and employed as active antibacterial agents in nanotechnology. This is because biogenic synthesis is simple and

environmentally friendly. Such nanoparticles have shown positive antibacterial activity against *S. aureus* bacterial strains and other antibacterial strains (Rahmat M *et al,* 2021).

2.8.1.2. Antifungal activity

Prevalence of fungal infections and fungal contamination has been at the forefront of worldwide safety affairs in the last few years. Taking the food industry as a notable example, fungal contamination cannot only cause the deterioration of product quality, and economic loss but also severely threaten food safety and public health. Manganese oxide nanoparticles s exhibits good antifungal activity due to their unique nano-properties, including excellent bioavailability and self-sterilization (Sun *et al*., 2018). The antifungal activity of MnO_2NPs was evaluated along with common antibiotics (e.g. ciprofloxacin, ampicillin, fluconazole, and amphotericin B). Their inhibitory efficiency can be enhanced in combination with MnO_2 NPs, which could reduce the overuse of antibiotics (N. Sharma *et al*., 2016).

Barad *et al*. have shown that MnO_2 NPs coated with chitosan-linoleic acid have significant efficacy compared with fluconazole in inhibitory action on the growth and biofilm formation of *C. albicans* (Gharagozloo *et al*., 2015). It is worth noting that many filamentous fungi can produce secondary metabolites known as mycotoxins, which can induce immune suppression, as well as embryonic and even carcinogenic effects on human health. Thus, the most important application value of MnO_2NPs lies in blocking and inhibiting the synthesis of mycotoxins (Savi *et al*., 2013).

2.8.2. Biomedical applications

Manganese-based nanoparticles have recently been employed extensively in theranostics applications. Their unique physical and chemical features, notably their high surface-to-volume ratio, make them effective drug delivery platforms. Manganese nanoparticles are unique in that they may be employed as chemotherapeutic drug delivery systems.

In addition to its use in drug delivery systems, nanostructured manganese dioxide has applications in photodynamic treatment, bio imaging, and cancer diagnosis. Tumour microenvironments are well-known for their high acidity and glutathione content. The tumour microenvironment may affect several cancer treatments now in use. As a result, manganese

nanoparticle drug delivery systems can be modified based on the notion of pH and glutathione responses to overcome toxicity (Hueso JL. *et al*, 2022).

2.8.3. Bio sensing Applications

Biosensing is great importance for early diagnosis and accurate theanostics. MnO_2 NPs has unique fluorescence quenching properties, catalytic properties, and intrinsic paramagnetic properties. According to the different detection mechanisms, MnO_2-based nanomaterials have been widely used to construct various bio sensing devices, such as fluorescent biosensors, colorimetric biosensors, chemiluminescence biosensors, MRI contrast agents, electrometric biosensors, and so on (Yudong Sun *et al*,2022).

3. Materials and Methods

3.1. Study Sites Description

The *D.alata* plant leaves used in this study were collected from Jimma zone, Oromia region. Synthesis of MnO_2NPs was done at the Department of Applied Chemistry research laboratory at ASTU. The characterization of the synthesized MnO_2 nanoparticles was done at Department of Applied Biology and Materials Science and Engineering in Adama Science and Technology University, Department of industrial Chemistry in Addis Ababa Science and Technology University, and department of Chemical Engineering in Bahir Dar University. The antibacterial and antifungal activities of MnO_2 NPs were done at the Institute of Pharmaceutical Science (IPS) laboratories in Adama Science and Technology University.

3.2. Chemicals and Reagents

All reagents and chemicals are used for this study analytical grade were Potassium permanganate ($KMnO_4$, analytical reagent, Trust Chemicals), Ethanol (C_2H_5OH, 96%, Fmd, Ethiopia), distilled water, Wagner's reagent (Iodine, I_2, 98.5%, Loba Chemical Pvt.Ltd), Sodium hydroxide(NaOH), Ferric Chloride ($FeCl_3$, 97%, Sigma-Aldrich), Chloroform ($CHCl_3$, 99.8%, Blulux), Sulfuric acid (H_2SO_4, 98 %, Sigma-Aldrich), Molten Hilton Agar (MHA). All the chemicals and reagents used for the preparation of MnO_2NPs were purchased from the local market in Addis Ababa.

3.3. Materials and Instruments

The equipment and apparatus required for MnO_2NPs synthesis were: Beaker, hot plate with a magnetic stirrer, magnetic bar, pH meter, micro oven, filter paper and funnel. petri dish, aluminium foil, mechanical grinder, centrifuge (LC-O4C), measuring cylinder, centrifuge tube, furnace (SX-2.5-10 BOX Type Resistance Furnace), refrigerator, crucible tongs, test tube rack, test tubes, dropper, volumetric flask (100, 250, and 500 mL), evaporating dish and electronic balance. Some of the instruments that were used in this study were XRD (XRD-7000, Shimadzu Co., Japan), UV–Vis spectroscopy (V-770 Dual-beam UV-VIS Spectrometer, Azzota Corp., USA), SEM (model JEOL JCM-6000plus, Japan) and FTIR (FT/IR-6600 type A, JASCO).

3.4. Methods

3.4.1. Preparation of *D. alata* plant leaf extract

Firstly, the leaf was washed tap water followed by cleaning with distilled water and allowed to dry at room temperature under a shadow area until the moisture content was removed and ready for fine grinding. Then, the extraction was carried out by taking 15g of the dried leaf powder into a 1000 mL beaker into which 600 mL distilled water (DH_2O) was added (Figure 5). Then the content was covered with aluminium foil and heated at a constant temperature of 60 ℃ for 1 hour (Ramesh P. *et al*., 2023). Then the extracted suspension was allowed to cool at room temperature followed by filtering. Finally, the plant extract solution was stored at 4 ℃ for further use in the synthesis of the Manganese dioxide nanoparticles.

Figure 5: Preparation of *Dioscorea alata* plant leaf extract.

3.4.2. Phytochemical screening of *D.alata* plant leaf extract

The *Dioscorea alata* plant leaf extract was subjected to assessment for the existence of the phytochemicals by using the following reported standard methods.

3.4.2.1. Test for Flavonoids

1mL plant Extract aqueous solution was taken and added 2mL 10% ferric chloride solution showed dark green precipitate. The color observed confirms the presence of flavonoids.

3.4.2.2. Test for Alkaloids (Wagner's test)

1 mL plant extract 1-2 drops of Wagner's reagent (Along the sides of test tube) a brown/reddish precipitate formed indicative of the presence of alkaloids. (Singh & Kumar, 2017).

3.4.2.3. Test for Saponins

2 mL of the plant extract and 5 mL of distilled water were combined and agitated. Then, the formation of foam confirmed the presence of saponins (Sileshi Dubale, *et al*, 2023).

3.4.2.4. Test for Tannins

2 mL of plant extract and 0.1% Ferric chloride was added to the mixture; which was then observed for blue-black coloration indicating the presence of tannins(Sileshi Dubale, *et al*, 2023).

3.4.2.5. Test for Phenol

5 mL of the extract was taken into a test tube and 3drop of 2 % of $FeCl_3$ was added to an extract drop by drop wisely showed bluish black colour due to the presence of phenols in the plant leaf extract (Sileshi Dubale, *et al*, 2023).

3.4.2.6. Test for Terpenoids

4 mL of plant extract was dissolved in the 3 mL of chloroform. Then, 2 mL of concentrated sulphuric acid was added confirm reddish brown (Altemimi *et al*., 2017).

3.4.2.7. Test for Glycosides

Adding 1 mL of distilled water and NaOH to 0.5 mL of plant extract, the formation of a yellowish colour indicated the presence of glycosides (Sileshi Dubale, *et al*, 2023).

3.4.2.8. Test for Steroids

5 mL of the extract was combined with 2 mL of chloroform and 1 mL of sulfuric acid, and the formation of the bilayer (red top layer and greenish bottom layer) reveals the presence of steroids (Sileshi Dubale, *et al*, 2023).

3.4.3. Green synthesis of MnO_2 nanoparticles

In this study the synthesis MnO_2NPS using *D. alata* plant leaf extract was carried out. The details of the procedures utilized during the synthesis were presented as follows: First 0.1M of potassium permanganate solution was prepared. The synthesis method was carried out using three different volume ratios of plant leaf extract and precursor salt: The first mixture was made up of 100 mL of 0.1 M potassium permanganate solution was mixed with 100 mL of *D.alata* leaf extract that is in1:1 ratio, the second case consist of 200 mL of 0.1 M potassium permanganates solution was mixed with 100 mL of *D.alata* that was 2:1 ratio, and in the third case 100 mL of 0.1 M of potassium permanganates solution was mixed with 200

mL of *D.alata* (1:2) in 1000 mL beaker for each ratio (Figure 6). Then the three samples were continuously stirred for about two hours on a magnetic stirrer. The pH of the solutions was checked using a pH meter. The PH of 1:1 ratio was 8.65, 1:2 ratios was 8.15 and that of 2:1 ratio was 8.80. Then after, the formed suspensions were kept in a refrigerator overnight for separation. The suspensions were centrifuged at 1000 revolutions per minute (rpm) for 15 min to obtain nanoparticles. Then each of the samples were washed a minimum of three times followed by washing with DH_2O and ethanol. Finally, the dried samples were kept for characterizations.

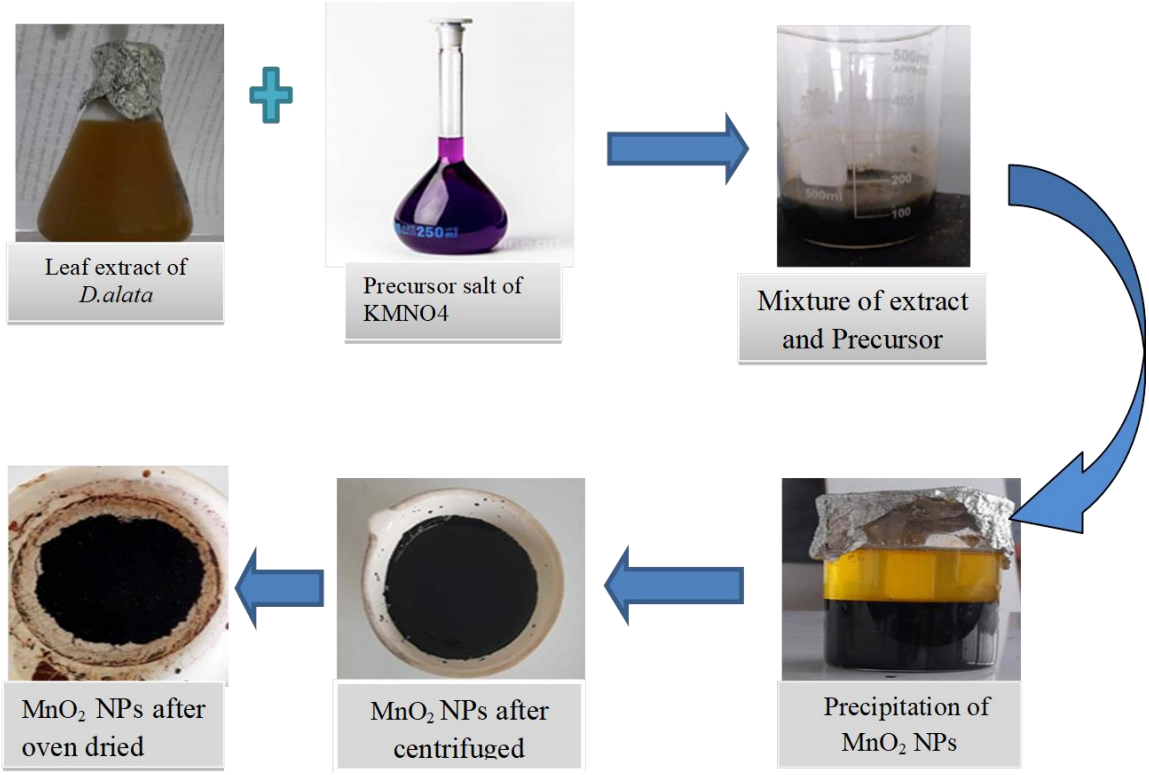

Figure 6: Schematic diagram for synthesis of MnO_2 nanoparticles by a green method.

3.5. Characterization of synthesized MnO_2NPs

Characterization of the synthesized sample is important in order to evaluate the functional aspects of the synthesized particles (Sanchez-Botero L *et.al*, 2017). Characterization of the sample was performed using a variety of analytical techniques, including UV-Vis spectroscopy, Powder X-ray Diffraction (XRD), Fourier transform infrared spectroscopy (FTIR) and scanning electron microscopy (SEM).

The optical properties of MnO_2 NPs was determined by the aid of UV- Visible spectroscopy (UV-Vis) in the wavelength range from 200-800nm.The functional group MnO_2 NPs was

determined by Fourier Transform-Infrared Spectroscopy (FT-IR) in frequency range from 400-4000cm^{-1}. The morphology of MnO_2 NPs was investigated with scanning electron microscope (SEM). Phase composition and purity of the phases MnO_2 NPs was observed by X-ray diffraction (XRD).

3.5.1 Characterization of MnO_2 NPs using XRD

XRD analysis is a primary technique commonly used for the identification of crystal structures, chemical composition, and purity of the phases (Shafiei A *et.al*, 2018).

A small amount of the synthesized MnO_2 NPs powder was taken and characterized using XRD. The crystalline structure of the green synthesized MnO_2 NPs was investigated. The crystallite size of the MnO_2 NPs was calculated using Debye Scherer formula.

$$D= \frac{0.94\lambda}{\beta cos\theta} \qquad (1)$$

Where D is the crystallite size, λ = 1.54 A^0 is the X - ray source wavelength, β is the full width at half maximum intensity (FWHM) of a peak, and θ is the peak position. To study effects of calcination, three of MnO_2 samples (1:2, 1:1 and 2:1) were calcined at 450^oC and other three samples (1:2, 1:1 and 2:1) were used uncalcined.

3.5.2. Characterization of MnO_2 NPs using UV-Vis Spectrophotometer

UV-Vis spectroscopy is a very useful and reliable technique for the characterization of synthesized MnO_2 NPs. It is mainly used to determine the optical property of the samples (eg. band gap energy) (Yahya S *et.al*, 2018). A small amount of the green synthesized MnO_2 NPs was taken and characterized using UV-Vis spectroscopy. The band gap of the synthesized sample was calculated as

$$Eg = \frac{hc}{\lambda} \qquad (2)$$

Where Eg is energy band gap, h is planks constant, c is speed of light and λ is the maximum wavelength of the synthesized NPs.

3.5.3. Characterization of MnO_2NPs using Fourier Transform Infrared (FTIR) spectroscopy

Fourier Transform Infrared (FTIR) spectroscopy is very powerful technique which provides fingerprint information and determines the functional group. The characterization of MnO_2 NPs was performed by putting the powder of the synthesized sample on KBr plate and the spectral data was recorded in IR region at the scanning range of 4000 - 400 cm^{-1} (Yahya S *et.al*,2018).

3.5.4. Characterization of MnO_2 NPs using Scanning Electron Microscopy

Scanning Electron Microscopy (SEM) is one of the most widely used technique to study surface morphology of materials. In addition to surface morphology, the SEM analysis can also be used to study size, and dispersion of MnO_2 NPs. Samples for SEM analysis were selected based on XRD data. This characterization reveal the agglomerations of individual MnO_2 particles and surface structure of MnO_2 particles. Then main information obtained from SEM was the morphology and surface structure of MnO_2 NPs (Hoseinpour V *et.al*, 2018).

3.6. Procedures for the antimicrobial activity analysis of the synthesized MnO_2 NPs

3.6.1 Disc diffusion method for Antimicrobial susceptibility testing

The purpose of the Kirby-Bauer disk diffusion susceptibility test was to determine the sensitivity or resistance of pathogenic aerobic and facultative anaerobic bacteria to various antimicrobial compounds. Determination of bacterial resistance to antimicrobials is an important part of the management of infections in patients. The disk diffusion method of Kirby and Bauer has been standardized and is a viable alternative to broth dilution methods for laboratories without the resources to utilize the newer automated methods for broth micro dilution testing.

When a 6-mm filter paper disk impregnated with a known concentration of an antimicrobial compound is placed on a Mueller-Hinton (MH) agar plate, immediately water is absorbed into the disk from the agar. The antimicrobial begins to diffuse into the surrounding agar. The

rate of diffusion through the agar is not as rapid as the rate of extraction of the antimicrobial out of the disk, therefore the concentration of antimicrobial is highest closest to the disk and a logarithmic reduction in concentration occurs as the distance from the disk increases. The rate of diffusion of the antimicrobial through the agar is dependent on the diffusion and solubility properties of the drug in MH agar and the molecular weight of the antimicrobial compound. Larger molecules will diffuse at a slower rate than lower molecular weight compounds. These factors, in combination, result in each antimicrobial having a unique breakpoint zone size indicating susceptibility to that antimicrobial compound (Hudzicki *et al*., 2016).

3.6.2. Preparation of McFarland standard

McFarland standards are suspensions of either barium sulfate or latex particles that allow visual comparison of bacterial density. A 0.5 McFarland standard is equivalent to a bacterial suspension containing between 1 x 10^8 and 2 x 10^8 CFU/ml of *E. Coli.*

3.6.3. Preparation of Mueller-Hinton plate

A 39 g of MH agar was added into 1L of distilled water. The agar was boiled to dissolve and sterilized at 121^{o}C at 15psi for 15 minutes and poured into sterile Petri plates Allow a MH agar plate (one for each organism to be tested) to come to room temperature (Hudzicki *et al*., 2016).

Since the surface of the agar was visible liquid, set of the plate was inverted, and ajar on its lid allow the excess liquid to drain from the agar surface and evaporate. Plates were placed in a 35°C incubator or in a laminar flow hood at room temperature until dry (usually 10 to 30 minutes). Finally appropriately each MH agar plate was labeled for each organism tested.

3.6.4. Antibacterial activity

The antibacterial activity of the synthesized NPs was evaluated against Gram-positive and Gram-negative bacteria using the standard disc diffusion method (Humphries et al., 2018). The bacterial strains that were used for the antibacterial study were two gram posetiv (*Escherichia coli, Pseudomonas aeruginosa) and two gram negative(Staphylococcus aureus, E. Faecalis).* The first step involved the preparation of Mueller-Hinton agar solution, which was subsequently sterilized. Following sterilization, the agar solution was poured in to

previously sterilized petri dishes and allowed to solidify. The inoculum was spread uniformly onto each petri dishes using sterile cotton swab. Next, sterilized discs were added in to different solutions of synthesized NPs along with different concentration (100, 50, 25 and 12.5 μg/mL). The discs containing the NPs were taken out of the solution and placed to each solidified Petri dishes. Negative and positive controls were also used, where Dimethyl sulfoxide (DMSO) was used as the negative control, and ciprofloxacin was used as the positive control. The Petri dishes were then left at room temperature for 30 minutes for proper diffusion and incubated at 37℃ for 24 hours for each bacterium. After 24 hours, the plates were taken out from the incubator, and the inhibition zones were measured using a millimetre ruler.

3.6.5. Antifungal activity

The Antifungal activity studies were carried out on one fungal strains *Candida albicans*. The study was carried out by using the disc diffusion method and the fungal growth was monitored by measurement of optical density of solution compared with a 0.5 McFarland standard solution and estimation of colony-forming units (CFUs) on solid growth. The agar solution was poured into sterilized petri dishes and allowed to solidify. The inoculum was spread uniformly onto each petri dishes using sterile cotton swab. Next, sterilized discs were added in to different solutions of synthesized NPs along with different concentration (100, 50, 25 and12.5 μg/mL). The discs containing the NPs were taken out of the solution and placed to each solidified Petri dishes. Negative and positive controls were also used, where Dimethyl sulfoxide (DMSO) was used as the negative control, and Gentamicin was used as the positive control. The Petri dishes were then left at room temperature for 30 minutes for proper diffusion and incubated at 37℃ for 24 hours. After 24 hours, the plates were taken out from the incubator, and the inhibition zones were measured using a millimetres ruler.

4. Results and Discussion

4.1. Phytochemical Screening of *D.alata* leaf Extract.

The phytochemical constituents of the *D.alata* plant extract was screened using various standard methods. In the present study, the qualitative phytochemical analysis of the aqueous leaf extracts of *D.alata* was carried out (Sileshi Dubale, *et al*, 2023). The results of the screening have revealed that *D.alata* leaf extract was rich in different phytochemicals (Table 1 and Figure 7) with different functional groups that might act as a capping agent during the synthesis of the MnO_2 NPs.

According to previous reports (Harborne and Baxter, 1995; Kokate *et al*., 2003), standard qualitative methods were carried out in order to investigate the resident phytochemicals like alkaloids, carbohydrates, flavonoids, glycosides, phenols, saponins, tannins, terpenoids, anthraquinones, and triterpenoids from *D.alata*. The results of phytochemical screening in this study revealed the presence of Alkaloid, Glycosides, Tannin, Flavonoid, Phenol, Saponins, Terpenoid and the absent of steroid. These phytochemicals containing OH functional groups possess lone pairs of electrons. These lone pairs of electrons in the phytochemicals play role of capping and stabilising agent in nanoparticle synthesis.

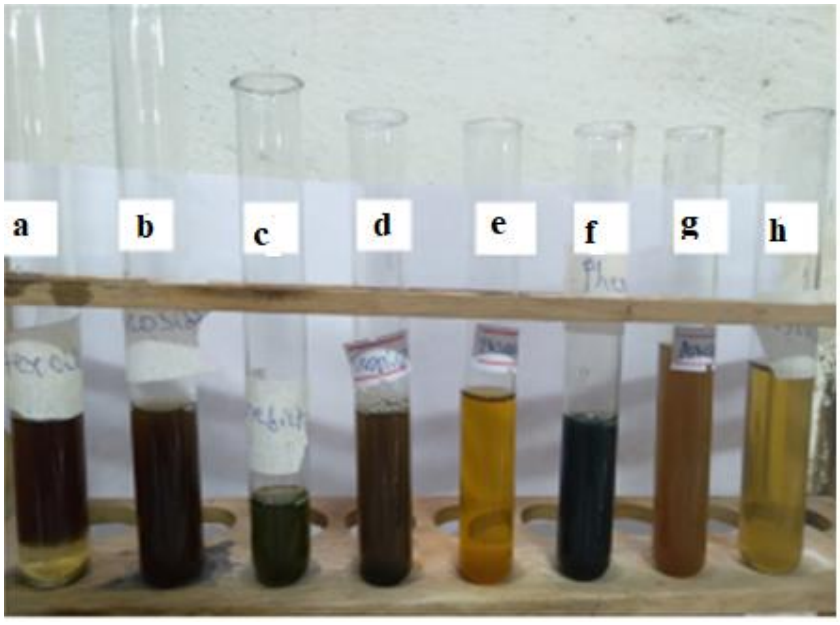

Figure 7: Phytochemical test for aqueous extract of *D.alata* leaf denoted by (a) for steroids, (b) for alkaloids (c) for tannins (d) for flavonoids (e) for Glycosid, (f) for phenol, (g) for saponins and, (h) Terpenoid.

Table 1*:* Results of phytochemicals screening of aqueous extracts of *Dioscorea alata.*

Sample code	Secondary Metabolite	Results	Colors observed
a	Steroids	-	No red color with greenish bottom layer
b	alkaloid	+	Redish-brown precipitate
c	Tannins	+	greenish – black
d	Flavonoids	+	Dark green
e	Glycosid	+	yellowish
f	phenol	+	Bluish-black
g	Saponins	+	Stable persistent foam
h	Terpenoid	+	Redish browen

4.2. Characterizations

4.2.1. X-Ray Diffraction (XRD) of MnO_2NPs analysis

The analysis of a crystal phase and average crystalline size of MnO_2 nanoparticles synthesized through the green method using *D.alata* leaf extract was conducted using X-ray diffractometer at room temperature. MnO_2 NPs were formed from the reduction of potassium permanganates in the presence of *D.alata* leaf extract, which acts as a reducing, stabilizing, and capping agent. From the six different samples of MnO_2 NPs characterized using XRD, the three were calcined (with sample codes 1:2C, 1:1C and 2:1C) at 450^oC and other three were uncalcined (with sample codes 1:2unC, 1:1unC and 2:1unC).

In Figure 8, the XRD peaks appeared at 2θ value of 12.8°, 18.04°, 28.86°, 36.24°, 41.98°,49.82°,56.08°, 60.18°, and 69.62°, corresponds to (110), (200), (310), (400), (301), (411), (600), (521) and (541) crystal planes for calcinated samples of (1:2,1:1,2:1) confirmed the presence of MnO_2 NPs (J.; Liu *et al*,2019 and X.; Li *et al*, 2018). The high intensity of XRD peaks at (110), (200), (310), (400), (411) and (521) shows high crystallinity for calcinated samples and low intensity of peaks at mentioned crystallite planes shows low crystallinity of uncalcinated samples of MnO_2 NPs.

Crystal structure of the synthesized NPs were found to be the alpha phase (α-MnO_2) with tetragonal structure, corresponding to the standard card number JCPDS (No. 044-0141) and matched with previous report(Kerkar RD, *et al* ,2020) with few impurities. The average grain size of the MnO_2 nanoparticles was calculated from the intense peaks using Debye-Scherer's formula and presented in the following Table 2. The average size for the different volume ratios (1:2C, 1:1C and 2:1C) and (1:2unC, 1:1unC and 2:1 unC) was found to be 16.73nm, 9.60nm , 16.90 nm. and 7.13nm,5.72nm, and 7.76nm , respectively.

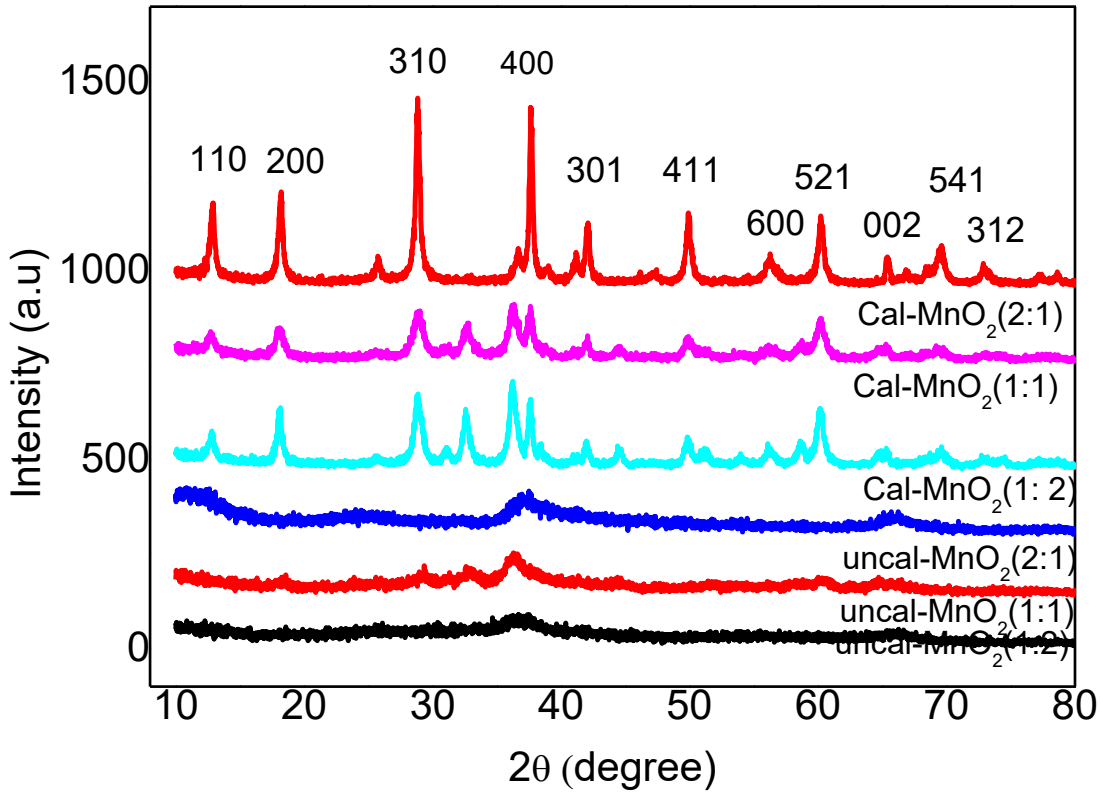

Figure 8: XRD patterns of MnO_2 nanoparticles synthesized under different ratios of potassium per manganese salt and *Dioscorea alata* leaf extract.

The result showed that the crystallinity of the biosynthesized MnO_2NPs has decreased from 2:1 through 1:2 and to 1:1 ratio. This is due to the fact that the greater amount of the plant extract used during the synthesis process results in effective capping and stabilizing the synthesized nanoparticles and hindered from aggregation. As shown in Table 2 the average crystallite sizes of uncalcinated MnO_2 NPs synthesized using 1:1, 1:2 and 2: 1 volume ratios of precursor salt and plant extract samples are less than their corresponding calcinated MnO_2 NPs. This may also be due to the high concentrations of biomolecules from plants that remain

in the uncalcinated NPs that could highly stabilize the nanoparticles by capping and hinders further crystal growth (Meron Girma *et al*,2020).

Table 2*:* XDR structural parameters of prepared MnO_2 nanoparticles

Calcined																
1:2 MnO_2 nanoparticle(α)						**1:1 MnO_2 nanoparticle (α)**						**2:1 MnO_2 nanoparticle (α)**					
h k l	Degree		FWHM (β)		Size (nm)	h k l	Degree		FWHM (β)		Size (nm)	h k l	degree		FWHM (β)		Size (nm)
	2θ	θ	degree	radian			2θ	θ	degree	radian			2θ	θ	degree	radian	
110	12.8	6.4	0.40	0.006	20.372	110	12.72	6.36	0.76	0.013	10.922	110	12.92	6.46	0.66	0.011	12.347
200	18.04	9.02	0.58	0.010	14.144	200	18.06	9.03	0.98	0.017	8.403	200	18.22	9.11	0.50	0.008	16.420
310	28.86	14.43	0.66	0.011	12.666	310	28.88	14.44	0.92	0.016	9.104	310	28.84	14.42	0.40	0.007	20.898
400	36.24	18.12	0.76	0.013	11.244	400	36.36	18.18	1.52	0.026	5.708	400	37.62	18.81	0.37	0.0065	23.288
301	41.98	20.99	0.42	0.0073	20.702	301	42.06	21.03	0.44	0.0076	19.884	301	42.1	21.05	0.46	0.0080	18.890
411	49.82	24.91	0.24	0.0042	37.0137	411	49.80	24.90	0.92	0.016	9.716	411	49.90	24.95	0.48	0.0084	18.527
600	56.08	28.04	0.82	0.0143	11.166	600	56.00	28.0	0.78	0.0136	11.749	600	56.2	28.1	0.88	0.0154	10.380
521	60.18	30.09	0.76	0.0132	12.348	521	60.12	30.06	0.94	0.0164	9.933	521	60.2	30.1	0.56	0.0097	16.804
541	69.62	34.81	0.90	0.0157	10.912	541	69.20	34.60	1.00	0.174	0.984	541	69.54	34.77	0.68	0.0118	14.554

Average Crystallite size				**16.73**	**Average Crystallite size**			**9.60**	**Average Crystallite size**		**16.90**
1:2 **MnO_2 nanoparticle(α) (uncalcined)**					1:1**MnO_2 nanoparticle(α) (uncalcined)**			2:1 **MnO_2 nanoparticle(α) (uncalcined)**			
400	36.66	8.14			400	36.28	5.30	400	36.75	8.60	
002	66.18	6.12			002	64.98	6.14	002	65.7	6.92	
Average Crystallite size 7.13						5.72			7.76		

4.2.2. Fourier Transforms Infrared Spectroscopy (FTIR) analysis

FTIR measurements were carried out to identify the possible bio-molecules responsible for the reduction of potassium per manganese and confirm formation of Mn-O bonds. Figure 9 shows the FTIR spectra of calcinated MnO_2 NPs (2:1C), uncalcinated MnO_2 nanoparticles (2:1), and leaves powder of *D.alata*.

The FTIR measurements were done to find functional groups of phytochemicals responsible for capping and stabilization of the Manganese oxide nanoparticles during synthesis of the NPs using leaf extracts of *D.alata.* The FT-IR spectra were recorded in the series of absorption bands between 4000 -400 cm^{-1} using the KBr pellet method at room temperature. Possible functional groups in biomolecules responsible for the reduction and capping agent of MnO_2NPs through particular bond vibrations peaks coming at defined wavenumbers was identified.

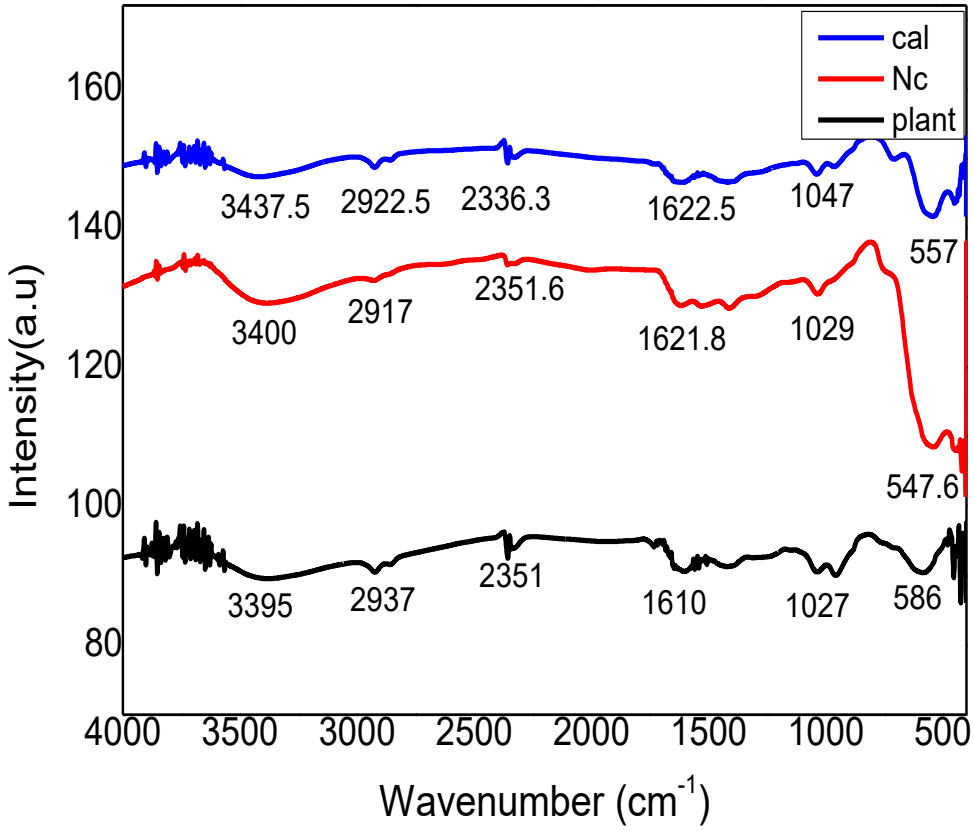

Figure 9: FT-IR spectrum for MnO_2 NPs calcined ($CMnO_2$), uncalcined MnO2NPs ($UCMnO_2$), and Dioscorea alata powder.

From Figure 9, different bands were observed at 3437.5 cm^{-1}, 2922.5 cm^{-1}, 2336 cm^{-1}, 1622.51 cm^{-1}, 1047cm^{-1}, 557 cm^{-1} in the calcined MnO_2 NPs. At 3400 cm^{-1}, 2917cm^{-1}, 2351.5cm^{-1} 1621.8 cm^{-1}, 1029 cm^{-1}, 547.6 cm^{-1} in the uncalcinated MnO_2NPs. At 3395cm^{-1}, 2937cm^{-1}, 2351 cm^{-1}1610 cm^{-1}, 1022 cm^{-1},586 cm^{-1} are from *D.Alata* powder.

The absorption bands located at 557 and 547 cm^{-1} (in calcined and uncalcined samples respectively) were attributed to the typical stretching vibrations of O–Mn–O bonds, which confirms the presence of MnO_2 in the prepared sample (Jaganyi D *et al*, 2013). The band at 1636 cm^{-1} is known as –OH bending vibration of a water molecule adsorbed on the surface of MnO_2 NPs, while a band at 1021 cm^{-1} is due to C–O stretching in molecule. These results indicate that some organic residues such as hydroxyl and carboxyl groups present on the surface of the MnO_2 nanoparticles. The bands at 2849 cm^{-1} and 2921 cm^{-1} are attributed to C–H stretching and bending vibrations. The broad band which appeared at 3433 cm^{-1} is the characteristic absorption for O–H–O of water and –OH stretching of the ethanol present in the system (M. Moeen *et al*, 2022).

Figure 9 shows the FT-IR spectra of calcined MnO_2NPs, uncalinated MnO_2NPs and plant powder. The O-H stretch appears in the spectrum as very broad and extending from 3437.5 cm^{-1}, 3400 cm^{-1} and 3395 cm^{-1} in calcined MnO_2NPs, uncalinated MnO_2NPs and plant leaf powder respectively. The band at 1622.5 cm^{-1}, 1621.8 cm^{-1} and 1610 cm^{-1}–OH bending vibration of adsorbed water molecule in calcined MnO_2NPs, uncalinated MnO_2NPs, and of phenolic phytochemicals in the plant powder. The bands at 2922.5 cm^{-1}, 2917 cm^{-1} and 2937 $cm^{-1}$are attributed to C–H stretching and bending vibrations. While a band at 1047cm^{-1}, 1029 cm^{-1} and 1027 cm^{-1} is due to C–O stretching in the phytochemicals.

4.2.3. UV-Visible Spectral Analysis

Figure 10, shows UV-Vis absorption spectrum of Manganese dioxide nanoparticles. Absorption spectrum was recorded for all samples in the range of 200-800 nm. Strong absorption bands were observed from UV–visible spectroscopy in between 250 and 360 nm for all samples (Figure 10).

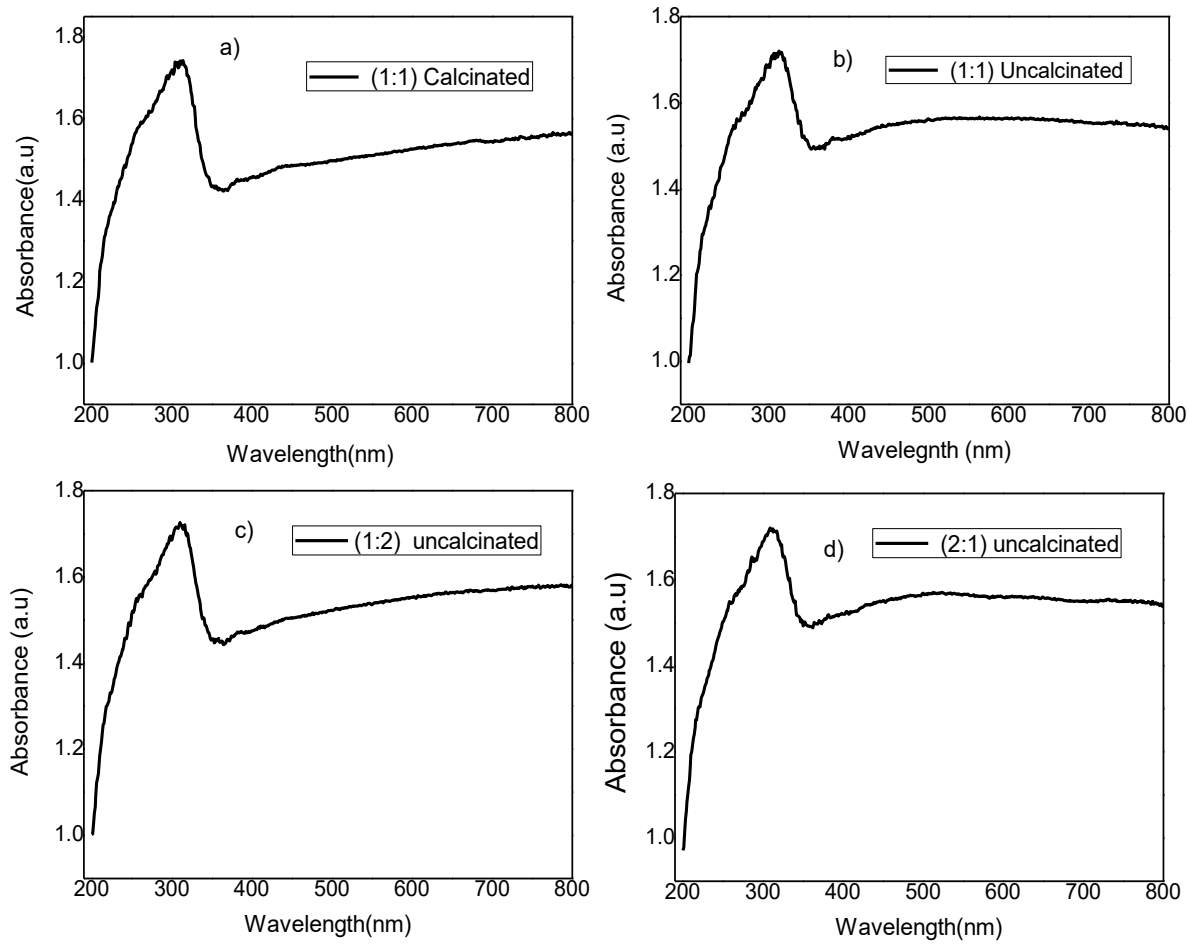

Figure 10: UV-Vis absorption spectra of a) (1:1) calcinated, b) (1:1), c) (1:2), and d) (2:1) uncalcinated samples of MnO_2 NPs synthesized by different volume ratios of plant extract to precursor salt solution.

The band gaps of MnO_2 NPs were extracted from Tauc plot (Figure 11) using Kubelka-Munk function (equation 3).

$$(\alpha h\nu)^{\frac{1}{n}} = B(h\nu - E_g) \quad \text{.....(3)}$$

Where B constant, n=1/2 (direct band transition), n=2 (indirect band transition)

Figure 11 (a-d) depicts Tauc plot of Manganese dioxide nanoparticles synthesized through green methods with four different volume ratios (1:2, 1:1, 2:1 and 1:1c) of precursor salt to plant extract. The bandgap energy (E_g) MnO_2 NPs were determined using the Tauc's plot method. With the Tauc plot in terms of the $(\alpha h\nu)^2$ versus $h\nu$ in Figure 11(a-d), the E_g for the green synthesized MnO_2 NPs such as uncalcinated (1:2), (1:1), and (2:1) and calcinated (1:1)

samples were determined to be 3.25, 3.09, and 3.05 eV respectively; and the E_g of the calcinated MnO_2 NPs was calculated to be 3.01 eV. Among uncalcinated samples, band gap shows decreasing trend with decrease of amount of plant extract used during synthesis. It also matches with average crystallite size of nanoparticles depicted in Table 2 in inverse relation. In line with the inverse relation of the band gap and size of nanoparticles, calcinated MnO_2 NPs with E_g of 3.01eV has average crystalline size of 9.60 nm (Agarwal.H *et al*, 2017,Chauhan.R *et al*, 2015 and Saravanan.M *et al*, 2018).

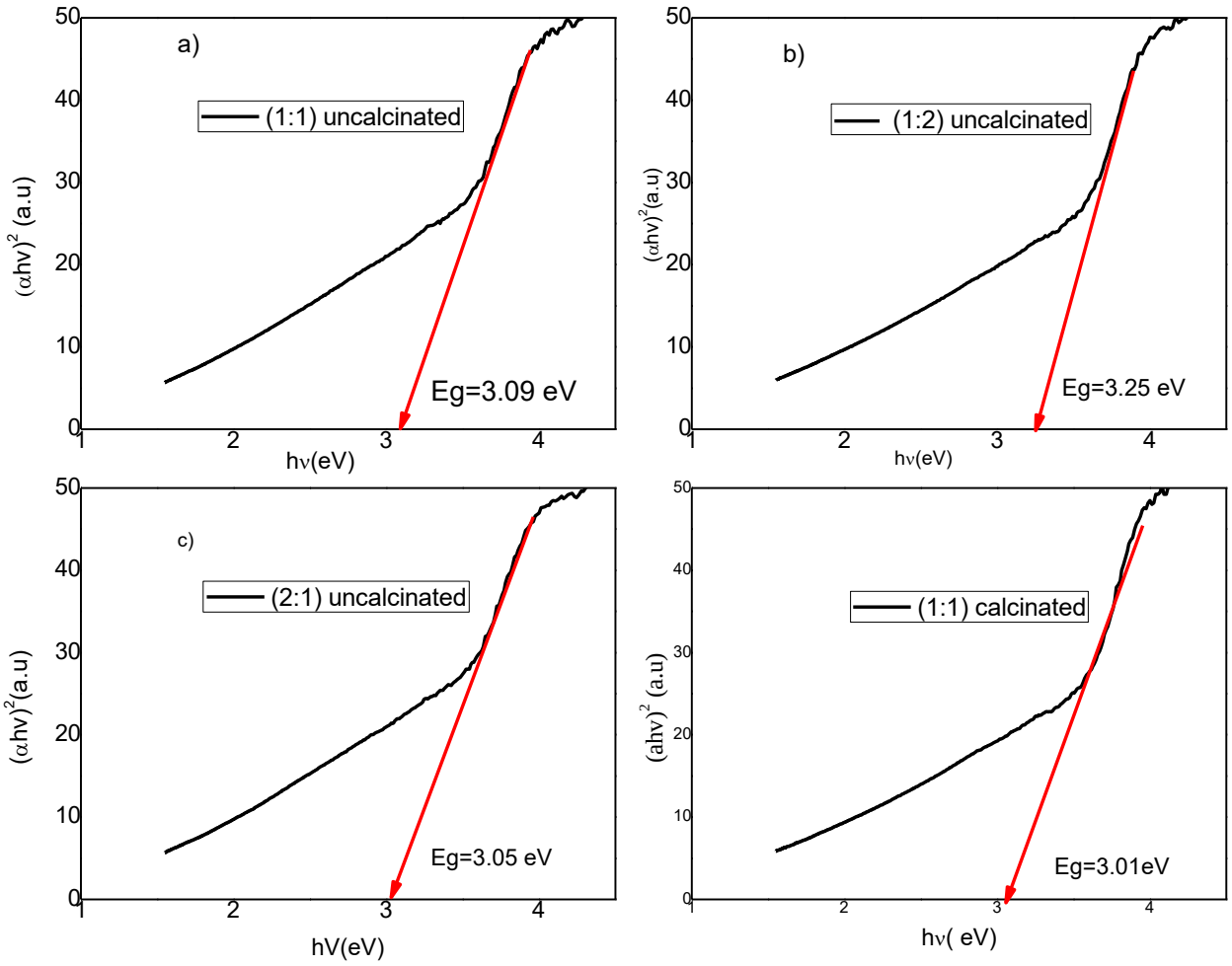

Figure 11: The energy band gap of a) uncalcinated (1:1), b) uncalcinated (1:2), c) uncalcinated (2:1) and d) calcinated (1:1) MnO_2 NPs determined using Tauc plot.

4.2.4. SEM Analysis

The study of morphological properties of the MnO_2 NPs was carried out using scanning electron microscopy (SEM); and the results obtained are shown in Figure 12 (a-f). From the SEM images it could be noted that the MnO_2 NPs are not homogenous and uniform in all

areas due to adhesion and agglomeration especially for the case of uncalcined MnO_2 NPs as presented in the Figure 12 (d-f). As can be seen, uncalcined MnO_2 NPs prepared in 2:1 volume ratio has shown high aggregation than other NPs synthesised with 1:2 and 1:1 volume ratios. In other words, the calcined MnO_2 NPs (1:2, 1:1 and 2:1 volume ratios) are less aggregated and agglomerated than uncalcined counter parts. The SEM images of calcined samples, Figure 12 (a-c) consist of agglomerations and aggregates of random shapes and size of MnO_2 nanoparticles due to the presence of Van der walls force. The particles are nearly spherical in shape. As shown in the figure, furnace morphology of 1:2, 1:1 and 2:1 calcined samples of MnO_2 NPs higher than uncalcined ones.

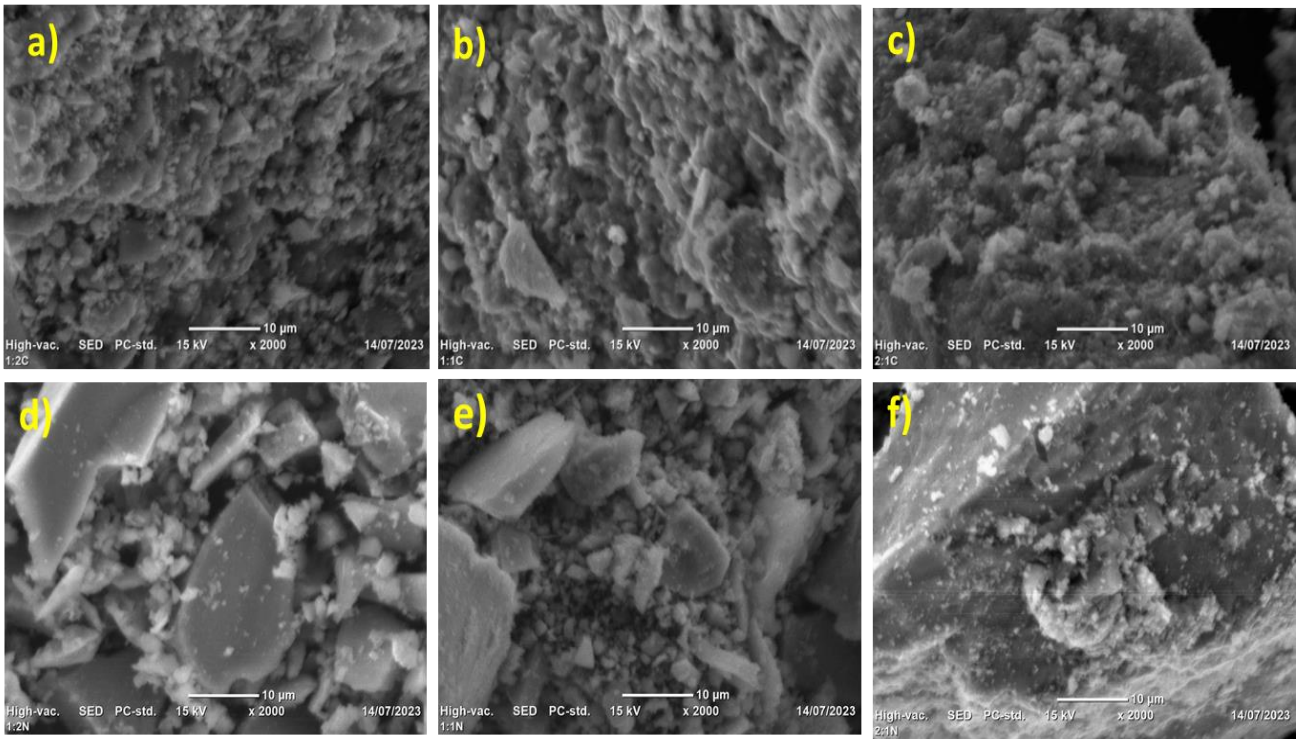

Figure 12: SEM images of α-MnO_2 NPs synthesized using different volume rations of precursor salt and *D.alata* , a) 1:2 (calcined), b) 1:1 (calcined), c) 2:1(calcined), d) 1.2(uncalcined), e) 1:1(uncalcined), and f) 2:1 (uncalcined).

4.3 Antimicrobial Activity Test of MnO_2 NPs

The synthesized MnO_2 NPs were tested for their antimicrobial activity against selected two gram-positive and two gram-negative bacterial strains. In addition the test was done on one fungal strain.

4.3.1 Antibacterial activity test of MnO_2NPs

The antibacterial effects of green synthesized MnO_2-NPs at different concentrations of the sample (100µg/mL, 50µg/mL, 25µg/mL and 12.5µg/mL) were evaluated against four bacterial strains, of which two were gram-positive (*S.aureus, and E. faecalis*) and two were gram-negative (*E.coli, and P. aerugin osa*,) were tested against pathogens using a disc diffusion methods.

The positive control, ciprofloxacin, was used against all the pathogens and the zone of inhibition values were measured as shown in Figure 13 and the results are presented in Table 3. The obtained result indicated that the synthesized MnO_2NPs have considerable antibacterial activity against all the four bacterial pathogens studied.

The difference in antibacterial activity is due to their difference in membrane structure (Gram-positive and Gram-negative). The gram-positive bacteria (*S. aureus* and *E. faecalis*) have a thick peptidoglycan layer and lack of outer membrane, whereas, the Gram-negative bacteria (*Escherichia coli, Pseudomonas aeruginosa)* have thinner peptidoglycan layer and surrounded by a lipid layer outside and have lipopolysaccharide outer membrane (Sundaraselvan & Darlin Quine, 2017).

Nanoparticles of MnO_2NPs exhibit attractive antibacterial properties due to increased specific surface area as the reduced particle size leading to enhanced particle surface reactivity and contact with the bacterial pathogenic. The smaller size of nanoparticles facilitates easy entry into the bacterial cell membrane and enables inhibition mechanisms to occur inside the cell. Increasing Manganese dioxides nanoparticle concentration and the smaller the particle size increases zone of inhibition.

In the antibacterial activity, initially, MnO_2NPs attach to the surface of the bacterial cell membrane and then penetrate the membrane of bacteria. After penetration, they inactivate the enzymes of the microbes, generating hydrogen peroxide. Hence bacterial cells will be dead

(Rahman S. *et al*, 2019). The proposed mechanism of antibacterial action of MnO_2 NPs on bacterial strains is given in Figure 13.

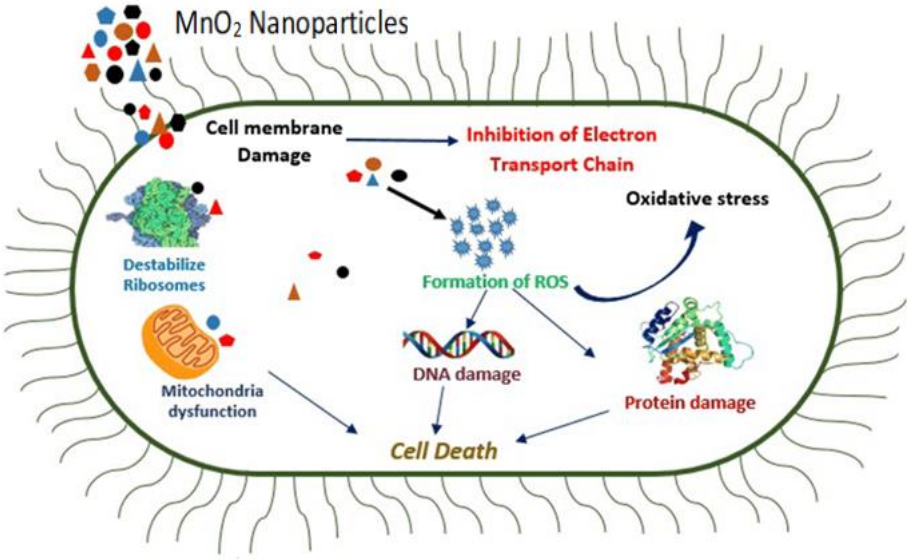

Figure 13*:* The proposed mechanism of antibacterial action of MnO_2 NPs on bacterial strains.

Table 3*:* Zone of inhibition (mm) of MnO_2 Nanoparticles against gram-positive and gram-negative bacterial strains.

Sample	Concentration (μg/ml)	*E. coli*	*S. aureus*	*P. aeruginosa*	*E. faecalis*
		(mm)	(mm)	(mm)	(mm)
MnO_2(2:1) (uncalcined)	100	15.33±0.58	11±1	10±1	16±2
	50	12.33±0.58	6.66±0.58	0	11±1
	25	8.66±1.15	0	0	9±0
	12.5	0	0	0	0
	(30)+vectrl (ciprofloxacin)	23.66±0.58	22.33±0.58	17±1	28.33±1.52
MnO_2(1:2) (uncalcined)	100	16±0	10.66±0.58	0	17.66±0.58
	50	10 .33 ± 0.58	8.66±0.58	0	13
	25	8.66±2.89	0	0	9±1
	12.5	0	0	0	0
	(30)+ve ctrl (ciprofloxacin)	28±1	26.33±0.58	17.66±0.58	29.33±0.58
MnO_2(1:1) (uncalcined)	100	14±1	11.33±0.58	0	16.66±0.58
	50	12.66±0.58	8.66±0.58	0	13±0.58
	25	10±0	0	0	10.33±0.58

	12.5	7.33±0.58	0	0	0
	(30)+ve ctrl (ciprofloxacin)	29.66±0.58	25.33±0.58	14.66±1.53	30.66±1.55
Dioscorea alata	100	12.33±0.58	12±0	9.66±0.34	14.33±0.58
	50	10.66±0.58	9.66±0.58	8.66±0.58	13±0
	25	8.66±0.58	0	0	9.33±0.58
	12.5	0	0	0	0
	(30)+ve ctrl (ciprofloxacin)	21±1	16.33±0.58	16.33±0.58	22±1
MnO_2(1:1) calcined	100	10.66±0.58	0	0	12±0
	50	9.66±0.58	0	0	10±0
	25	7.66±0.58	0	0	8±1
	12.5	0	0	0	0
	(30)+ve ctrl (ciprofloxacin)	21±1	16.66±0.58	15.33±0.58	22±1

Antibacterial activity results showed that green synthesized MnO_2 nanoparticle using *Dioscorea alata* leaf extract has exhibited antibacterial activity against both gram-positive (*S. aureus, E. faecalis)* and gram-negative (*E. coli, P. aeruginosa)* bacterial strains. As shown in figure 14, the uncalcined MnO_2 nanoparticles performed better antibacterial activity both gram-positive and gram-negative bacterial strain.

According to Table 3 MnO_2NPs for a 1:2 ratio at 100, 50, 25, 12.5 µg/mL concentration have zone of inhibition of 16, 10.33±0.58, 8.66 ±2.89,0 for gram negative (*E.coli*) and 0, 0, 0, 0, for gram negative (*P. aeruginosa*). Zone of inhibition of the gram positive (*S. aureus) was 10.66± 0.58,*8.66 *±0.58, 0, 0,* and the gram positive (*E. faecalis) was 17.66± 0.58,*13, *9* ±1,0 respectively. The positive control has shown the inhibition zone of 28±1, 26.33±0.58, 17.66±0.58, and 29.33±0.58 for *E. coli, S. aureus, P. aeruginosa and E. faecalis* respectively.

MnO_2 NPs for 1:1 ratio at 100, 50, 25 and 12.5µg/mL concentration have the zone of inhibition of the gram negative (*E.coli) was* 14±1, 12.66± 0.58, 10, 7.33± 0.58*, and that of the othe gram negative (P. aeruginosa*) was 0, 0, 0, 0 respectively. In the same way, zone of inhibition of the gram positive (*S. aureus) was 11.33± 0.58, 8.66± 0.58,0,0,* and that of another gram positive (*E. faecalis) was 16.66± 0.58,13, 10.33± 0.58,0* respectively. For the case of MnO_2 NPs (1:1), the positive control has exhibited the inhibition zone of 29.66±0.58,

25.33±0.58, 14.66±0.53, and 30.66±1.55 for *E. coli, S. aureus, P. aeruginosa and E. faecalis* respectively.

MnO_2 NPs for 2:1 ratio at 100, 50, 25 and 12.5µg/mL concentration have the zone of inhibition of gram negative (*E.coli) was,* 15.33± 0.58, 12.33± 0.58, 8.66± 1.15, 0 and that of the other gram negative (*P. Aeruginosa) was* 10± 1, 0, 0, 0 respectively. In the same way, zone of inhibition of gram positive (*S. Aureus)* was *11± 1, 6.66 ±0.58, 0, 0 and that of the other gram positive (E. Faecalis) was 16± 2, 11± 1, 9, 0 respectively.* In the case of MnO_2 NPs (2:1), the positive control has demonstrated the inhibition zone of 23.66±0.58, 22.23±0.58, 17±1, and 28.33±1.52 for *E. coli, S. aureus, P. aeruginosa and E. faecalis* respectively.

Dioscorea alata leaf powder at 100, 50, 25 and 12.5µg/mL concentration have zone of inhibition against gram negative (*E.coli)*) was 12.33± 0.58, 10.66± 0.58, 8,0 respectively. And that of the other gram negative (*P. Aeruginosa) was* 9.66± 0.34, 8.66 ±0.58, 0, 0 respectively. In the same way zone of inhibition of gram positive (*S. aureus) was 13, 9.66± 0.58, 0, 0 respectively and that of the other gram positive (E. faecalis) was 14.33± 0.58, 13,9.33*±0.58*, 0.* The positive control used *D. alata* has shown the zone of inhibition of 21±1, 16.33±0.58, 16.33±0.58, and 22±1for *E. coli, S. aureus, P. aeruginosa and E. faecalis* respectively.

MnO_2 NPs for calcined1:1 ratio at 100, 50, 25 and 12.5µg/mL concentration have the zone of inhibition of gram negative (*E.coli*) was, 10.66±0.58, 9.66±0.58, 7.66±0.58, 0 and that of the other gram negative (*P. Aeruginosa*) was 0,0,0,0 respectively. In the same way zone of inhibition of gram positive (*S. Aureus) was, 0, 0, 0,0 and that of the another gram positive(E. Faecalis) 12,10, 8 ±1,0* respectively. The zone of inhibition of the positive control agaist *E. coli, S. aureus, P. aeruginosa and E. faecalis* was found to be *21±1, 16.33±0.58, 15.33±0.58, and 22±1* respectively.

As shown in table 3 the uncalcinated MnO_2 nanoparticles performed better antibacterial activity on gram-positive than the gram-negative bacteria. Previous research report also indicated antibacterial activity of MnO_2 nanoparticles were greater on gram-positive than gram-negative bacteria (Tayel *et al*., 2011).

The reason for the difference in sensitivity between gram-positive and gram-negative bacteria might be attributed to the differences in morphological constitutions between these microorganisms. Gram-negative bacteria have an outer lipopolysacharide membrane and this makes the cell wall impermeable to antibacterial chemical substances. Gram-positive bacteria on the other hand are more susceptible having only an outer peptidoglycan layer which is not an effective permeability barrier. the cell walls of gram-negative bacteria are more complex in lay out than the gram-positive ones acting as a diffusion barrier and making them less susceptible to the antibacterial agents (Alonso *et al*., 2000).

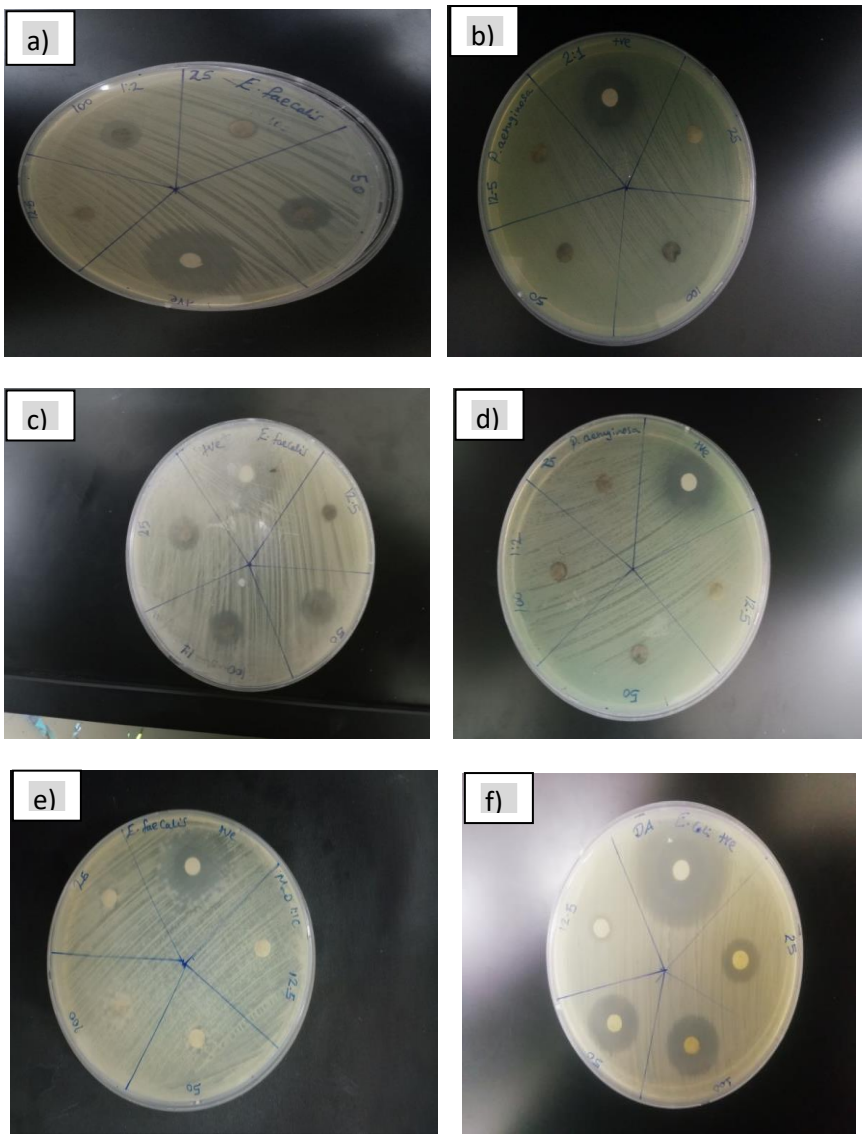

Figure 14: Zone of inhibition (mm) of MnO_2 NPs against a) E. faecalis at 1:2, b) P. aeruginosa at 2:1, c) E. faecalis at 1:1, d) P. aeruginosa at 1:2, e) E. faecalis at 1:1 calcinated nanoparticles and f) D.alata.

4.3.2 Antifungal activity

The antifungal activities of synthesized MnO_2NPs was evaluated for their antifungal effects against human pathogenic fungal strains *C. Albicans* different concentrations of the sample (100µg/mL, 50µg/mL, 25µg/mL and 12.5µg/mL) was tested against pathogens using a disc diffusion methods. The positive control of Gentamicin against the pathogens and the zone of inhibition values was measured as depicted in Figure 15 and the results given in Table 4. The analysis of the results indicated that the synthesized MnO_2 NPs has shown considerable antifungal activity.

Table 4: Zone of inhibition (mm) of MnO_2 Nanoparticles against fungal strain.

Sample	Concentration (μg/ml)	*C. Albicans* (mm)
MnO_2(2:1) (uncalcined)	100	14.33±0.58
	50	12.66±0.58
	25	7
	12.5	0
	(10)+ve ctrl (Gentamycin)	15
MnO_2(1:2) (uncalcined)	100	17.66±0.58
	50	14.66±0.58
	25	7
	12.5	0
	(10)+ve ctrl (Gentamycin)	20
MnO_2(1:1) (uncalcined)	100	15.66±0.58
	50	13.33±0.58-
	25	7±1
	12.5	0
	(10)+ve ctrl (Gentamycin)	15.33±0.58
Dioscorea alata	100	9±1
	50	7.33±0.58
	25	7.33±0.58
	12.5	0
	(10)+ve ctrl (Gentamycin)	13.66±0.58
MnO_2(1:1) calcined	100	11±1
	50	7.66±0.58
	25	7±1
	12.5	0
	(10)+ve ctrl (Gentamycin)	13.33

Antifungal activity results showed that green synthesized MnO_2 nanoparticle using *Dioscorea alata* leaf extract has exhibited strong antifungal activity against *C. Albicans.*

According to Table 4 MnO_2NPs for 1:2 ratio at 100, 50, 25 and 12.5µg/mL concentration have the zone of inhibition for *C. Albicans were* 17.66 ± 0.58, 14.66 ± 0.58, 7 *and* 0 *respectively*.

MnO_2 NPs for 1:1 ratio at 100, 50, 25 and 12.5µg/mL concentration have the zone of inhibition *for C. Albicans were* 15.66 ± 0.58, 13.33 ± 0.58, 7 ± 1 *and* 0 *respectively*.

MnO_2 NPs for 2:1 ratio at 100, 50, 25 and 12.5µg/mL concentration have the zone of inhibition *for C. Albicans were* 14.33 ± 0.58, 12.66 ± 0.58, 7 *and* 0 *respectively*.

MnO_2 NPs for calcined 1:1 ratio at 100, 50, 25 and 12.5µg/mL concentration have the zone of inhibition *C. Albicans* 11 ± 1, 7.66 ± 0.58, 7 ± 1 and 0 respectively.

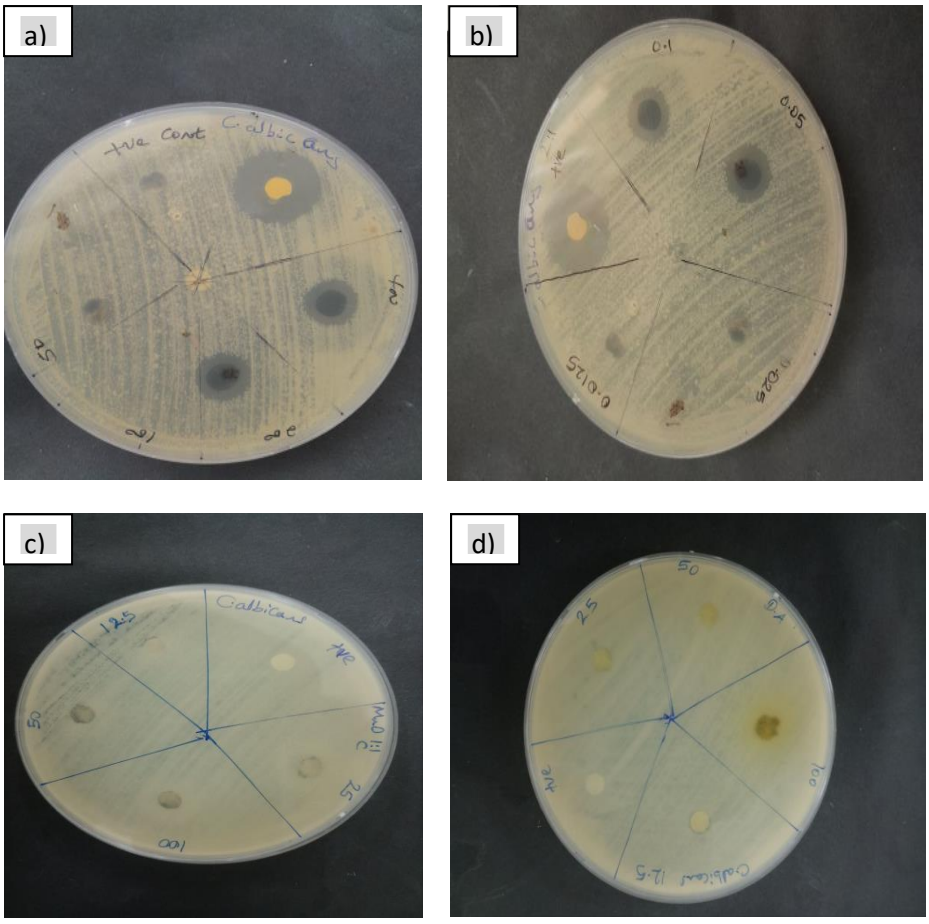

Figure 15: Zone of inhibition (mm) of MnO_2 against C. Albicans a) 1:1, b) 2:1, c)1:1 calcinated nanoparticles and d) *D.alata powder.*

D.A at 100, 50, 25 and 12.5µg/mL concentrations have the zone of inhibition *for C. Albicans* were 9 ± 1, 7.33 ± 0.58, 7.33 ± 0.58 and 0 respectively. The zone of inhibition for positive control (Gentamycin) against *C. Albicans* was 15, 20, 15.33 ± 0.58, 13.66 ± 0.58, and 13.33 mm for MnO_2(2:1) uncalcined, MnO_2(1:2) uncalcined, MnO_2(1:1) uncalcined, *D.alata, and* MnO_2(1:1) calcined samples respectively.

4.3.3. Anti-bacterial and Anti-fungal comparative study

Table 5 shows comparative antibacterial activities of green synthesized MnO_2 NPs against both gram-negative (*E. coli, P. aeruginosa*) and gram-positive (*S. aureus, E. faecalis*) bacterial strains with the findings of this work. As indicated in the table antibacterial zones of inhibition of synthesized MnO_2 NPs against *E.Coli* was 16 mm, and zone of inhibition of the nanopartilces against this bacterial strain was ranged from 11mm to 22 mm according to reports (Muhamed H. M *et al*, 2017, Naveen C. J *et al*, 2020, Naveen C. J. & Ekta J. *et al* 2020, Saod W. M.*et al*, 2022 and Ramesh P. *et al*, 2023). The zone of inhibition of synthesized MnO_2 NPs (16 mm) is in agreement with the reported values (11-22mm). Whereas MnO_2 NPs exhibited no antibacterial activity against the second gram negative bacterial strain (*P. aeruginosa*).

In the same way, zone of inhibition of synthesized MnO_2 NPs for gram positive bacterial strains of *S. aureus* and *E. faecalis* was measured to be 11 mm and 17.66 mm respectively. As indicated in Table 5, reported values of zone of inhibition of MnO_2 NPs against *S. aureus* ranges between 13 and 19 mm. Zone of inhibition of synthesized MnO_2 NPs against *S. aureus* (11mm) was closer to reported value of 13 mm. For the case of *E. faecalis*, synthesized MnO_2 NPs was shown the zone of inhibition of 17.66 mm, which is better than reported value (16 mm) (Mahlangeni N. T.*et al*, 2020).Concerning anti-fungal testing, the zone of inhibition of synthesized MnO_2 NPs was measured against the common fungal strain of *C. Albicans.* As depicted in Table 5, zone of inhibition of synthesized MnO_2 NPs was 17.66 mm. According to some reports (Jayandran M.*et al*, 2015, Shanshool S. *et al*, 2023), the zones of inhibition of MnO_2 NPs against *C. Albicans* were ranged between 16 mm and 19mm. Hence, antifungal activity of synthesized MnO_2 NPs against *C. Albicans* in this study is a good agreement with reported values as shown in the table.

Table 5: Comparison of Antibacterial and antifungal zone of inhibition of green synthesized MnO_2 NPs of this work with related reports (at 100 µg/ml of NPs concentration).

s.no	Nanoparticles	Bacterial strain	Zone of inhibition of Literature		Zone of Inhibition of this work		Fungal strain	Zone of inhibition of Literature		Zone of Inhibition) this work	
			References	Value (mm)	This work	Value (mm)		References	Value (mm)	This work	Value (mm)
1	*$MnO_{2\ (1:2)}$ uncalcinated*	*E.coli*	*Muhamed H. M et al, 2017, Naveen C. J et al, 2020, Naveen C. J. & Ekta J. et al 2020, Saod W. M.et al, 2022 and Ramesh P. et al, 2023*	*11, 12,18,19 & 21*	*This work*	*16*	*C. Albicans*	*Jayandran M.et al, 2015, Shanshool S. et al, 2023*	*16, & 19*	*This work*	*17.66*
2	*$MnO_{2\ (1:2)}$ uncalcinated*	*S.aureus*	*Saod W. M.et al, 2022, Muhamed H. M et al, 2017, Shanshool S. et al, 2023,& Jayandran M.et al, 2015*	*12,13,16,19*	*This work*	*11*					
3	*$MnO_{2\ (1:2)}$ uncalcinated*	*E.faecalis*	*Mahlangeni N. T.et al, 2020*	16	*This work*	*17.66*					
5	*$MnO_{2\ (1:2)}$ uncalcinated*	*P.aeruginosa*	*Saod W. M.et al, 2022 & Ramesh P. et al, 2023*	18	*This work*	*0*					

5. Conclusions

It is known that the green synthesis of MnO_2 nanoparticles is much safer and environmentally friendly as compared to chemical synthesis. In this study Potassium permagenta was used as a precursor and *Dioscorea alata* leaf extract as a capping and stabilizing agent to create MnO_2 nanoparticles. Formation of MnO_2 nanoparticles was confirmed by observation of brownish black colour during synthesis. The synthesized product was characterized and confirmed to be MnO_2NPs using UV–Vis absorption spectroscopy, X-ray diffraction (XRD), Fourier transform infrared spectroscopy (FT-IR), scanning electron microscopy (SEM). As confirmed from XRD, the size of MnO_2 nanoparticle was found to be in ranges of 9.60 – 16.90 nm which was obtained by varying reactant ratio by volume. Moreover, the *Dioscorea alata* leaf extract stabilized MnO_2NPs exhibited considerable antimicrobial activity against pathogenic bacteria and fungi which is comparable with that of standard antibiotics. Synthesized MnO_2 nanoparticles has demonstrated very good antibacterial zone of inhibition of 11mm, 16 mm and 17.66 mm against *S.aureus*, *E.coli* and *E.faecalis* respectively. MnO_2 nanoparticles also has shown anti-fungal zone of inhibition of 17.66 mm against fungal strain of *C. Albicans* Generally, the result in this study indicates that MnO_2 nanoparticles were effective both against gram positive bacterial strains (*S. aureus and E. faecalis)* and gram-negative bacterial strain (*Escherichia coli)*; and also found effective against strain (*C. Albicans*).

6. Recommendation

Despite the environmental advantages of using green chemistry based biological synthesis over traditional methods, some unresolved issues such as understanding of the mechanisms of action of plant extract during synthesis of nanoparticles. In the case of plant extracts, nanoparticle formation mechanisms vary between different plants species. Therefore, there is a need for more studies to evaluate and understand the actual plant dependent mechanisms. This is a grossly unexplored field and requires much more research investment to fully utilize green synthesis of metallic nanoparticles using biological entities. In particular, MnO_2 reduces the bacteria viability; however, the exact mechanism of its antibacterial activity has not been covered by this study so far. Therefore, investigations of mechanism of action (inhibition) MnO_2 nanoparticles against bacterial and fungal strains. In order to have better insight of whole antimicrobial activities of MnO_2 NPs, it is recommended to study antioxidant activity of the nanoparticles.

7. References

Agarwal, H.; Kumar, S. V.; Rajeshkumar, S. (2017) 'A review on green synthesis of zinc oxide nanoparticles - An eco-friendly approach' Resource-Efficient Technologies. 406-413.

Akbari S., Foroughi M. Mehdi .and Ranjbar M. (2018) 'Solvent-free Synthesis and Characterization of MnO_2 Nanostructures and Investigation of Optical Properties' Journal of Nanomedicine & Nanotechnology DOI: 10.4172/2157-7439.1000498.

Anastas P.T, Warner J.C.(1998) 'Green chemistry: Theory and practice' Oxford University Press, New York, 30.

Annu , Akbar. AliA., and Ahmed Shakeel Ahmed, (2018) ' Green Synthesis of Metal, Metal Oxide Nanoparticles, and Their Various Applications' Handbook of Ecomaterials, doi.org/10.1007/978-3-319-48281-1_115-1.

Arbab Mohammad Toufiq Fengping Wang Qurat-ul-ain Javed Quanshui Li Yan Li (2014) 'Hydrothermal synthesis of MnO_2 nanowires: structural characterizations, optical and magnetic properties' Appl. Phys. Vol. 116:1127–1132.

Areej Ahmed Mohammed, Adnan Raad Ahmed, Muhammad Hameed AL-TIMIMI, (2022) 'Structural, Optical and Thermal Properties of (PEG/PAA: MnO2) Nano Composites' Technium BioChemMed, Vol. 3, pp.107-119.

Awad M. A., Hadia N. M. A. (2018) 'Towards understanding the morphological, magnetic, optical and electrical properties of MnO2nanowires for magneto-and optoelectronic applications' Journal of Materials Science: Materials in Electronics vol. 29:20695–20702.

Awwad M., Albiss B., Ahmad L., (2014). 'Green synthesis, characterization and optical properties of zinc oxide nanosheets using Oleaeuro pea leaf extract' Adv. Mat.Lett. 5,520.

Chauhan, R.; Reddy, A. Abraham, J.(2015) 'Biosynthesis of silver and zinc oxide nanoparticles using *Pichia fermentans* JA2 and their antimicrobial property' *Appl. Nanosci.* **5**, 63–71.

Durail S.C. V., Kumar E., Muthuraj D., Jothy V. B.(2020) 'Investigation on Electrical and Structural, Properties of Manganese Dioxide Nanoparticles' Journal of Nano- and Electronic physics, Vol. 12, 03011.

Duran N, Marcato P.D, Duran M, Yadav A, Gade A, Rai M.(2011) ' Mechanistic aspects in the biogenic synthesis of extracellular metal nanoparticles by peptides, bacteria, fungi and plants' Applied Microbiology and Biotechnology, 90: 1609-1624.

Duran N, Marcato PD, Alves OL, De souza GI, Esposito E.(2005) 'Mechanistic aspects of biosynthesis of silver nanoparticles by several *Fusarium oxysporum* strains' Journal of Nanobiotechnology, 3: 1-17.

Ganeshan S., Ramasundari P., Elangovan A., Arivazhagan G. and Vijayalakshmi I. (2017) 'synthesis and characterization of mno2 nanoparticles: study of structural and optical properties' international journal of scientific research in physics and applied sciences vol. 5, pp.5-8

Gharagozloo, M., Kalantari, H., Rezaei, A., Maracy, M. R., Salehi, M., Bahador, A., Hassannejad, N., Narimani, M., Sanei, M. H., Bayat, B., & Ghazanfari, H. (2015). 'Clinical Study Immune-mediated cochleovestibular disease' *Bratislavsk LekRske Listy*, *116*(5), 296–301.

Haibinlu,Xueyang Zhang,ShakeuAhmed,WenqianqlangLi and LeiWan,(2021) 'Biogenic Synthesis of MnO_2 Nanoparticles With Leaf Extract of Viola betonicifolia for Enhanced Antioxidant, Antimicrobial, Cytotoxic, and Biocompatible Applications'Vol.12,. doi: 10.3389.

Harishkumal,Manisha and Poonamsangwan(2013) ' Synthesis and Characterization of MnO_2 Nanoparticles using Co-precipitation Technique'International Journal of Chemistry and Chemical Engineering,Vol.3,pp. 155-160.

Hendi A. H. Y., Al-Kuhaili M. F., Durrani S. M. A. 'Chemical and optical properties of MnO2 thin films prepared by reactive evaporation of manganese'International Journal of Research in Engineering and Technology, 5, 2321-7308

Jan Hudzicki, (2016) ‘ Kirby-Bauer Disk Diffusion Susceptibility Test Protocol’ American Society for Microbiology, 1-23.

Jayandran M., Haneefa M. M., Balasubramanian V., (2015) ‘Green synthesis and characterization of Manganese nanoparticles using natural plant extracts and its evaluation of antimicrobial activity’ Journal of Applied Pharmaceutical Science, 5 (12), 105-110.

Jayandran M., Haneefa M. M., Balasubramanian V., (2015) ‘Green synthesis and characterization of Manganese nanoparticles using natural plant extracts and its evaluation of antimicrobial activity’ Journal of Applied Pharmaceutical Science, 5 (12), 105-110.

Jino Affrald R, Nandhini M , Shoba Narayan (2023) ‘A comprehensive review of manganese dioxide nanoparticles and strategy to overcome toxicity’ Nanomed J. 10(1): 1-15.

Kavitha, K. S., Baker, S., Rakshith, D., Kavitha, H.U., Yashwantha, R. H. C., Harini, B. P. and Satish, S. (2013) ’Plants as green source towards synthesis of nanoparticles’ *Inter. Res. J. Biol. Sci.*, *6*, 66.

Khitam S. Shaker Alyaa H. AbdAlsalm (2018) ‘Synthesis and Characterization Nano Structure of MnO2 via Chemical Method’ , Engineering and Technology Journal, , 36, 946-950.

Kollur Shiva Prasad and Alakananda Patra ,(2017) ‘ Green synthesis of MnO_2 nanorods using Phyllanthus amarus plant extract and their fluorescence studies’,Green Process Synth , 6: 549–554

Mahlangeni N. T., Magura • J., Moodley R. • Baijnath H., Chenia H., (2020) ‘Biogenic synthesis, antioxidant and antimicrobial activity of silver and manganese dioxide nanoparticles using Cussonia zuluensis Strey’, Chemical Papers, 74, 4253-4265.

Mahsa Souri, Nasser Ghaemi, 2018, Green synthesis, characterisation, and photocatalytic activity of manganese dioxide nanoparticles’, Micro & Nano Letters, Vol. 13, pp. 1560–1563.

Matlack AS. (2001) ‘Introduction to green chemistry’ 3rd ed., Marcel Decker Publishers, New York. pp. 3-7.

Meron Girma Demissie, Fedlu Kedir Sabir, Gemechu Deressa Edossa,and Bedasa Abdisa Gonfa’(2020) ‘Synthesis of Zinc Oxide Nanoparticles Using Leaf Extract of *Lippiaadoensis* (Koseret) and Evaluation of Its Antibacterial Activity’ Journal of Chemistry Volume , 9.

Mohammed Areej A.AhmedA. Mohammed, Ahmed Adnan A. RaadR. Ahmed, Hameed Muhammad M. Hameed AL-TIMIMI. (2022) ‘Structural, Optical and Thermal Properties of (PEG/PAA :MnO2) Nano Composites’ Technium BioChemMed, Vol. 3, pp.107-119.

Moon S. A., Salunke B. K., Alkotaini B., Sathiyamoorthi E., Kim B. S., (2015) ‘Biological synthesis of manganese dioxide nanoparticles by Kalopanax pictus plant extract’ IET Nanobiotechnol. Vol. 9, 220–225.

Muhamed H. M., Jayandran M., Balasubramanian V. (2017) ‘Evaluation of antimicrobial activity of green-synthesized manganese oxide nanoparticles and comparative studies with curcuminaniline functionalized nanoform’Asian J Pharm Clin Res, 10(3), 347-352.

Naveen C. J., Ekta J., Ajay S., (2020) ‘Biological Synthesis, Characterisations and Antimicrobial activities of manganese dioxide (MnO_2) nanoparticles’ Research J. Pharm. and Tech. 13(1), 135-140.

Naveen C. J., Faisal S., Mohd S., Ajay S., (2020) ‘Antibacterial Activity, Characterizations, and Biological Synthesis of Manganese Oxide Nanoparticles using the Extract of Aloe vera’ Asian Pac. J. Health Sci., 7(3), 27-29.

Ngoan Thi Thao Nguyen, Luan Minh Nguyen, Thuy Thi Thanh Nguyen, Thuong Thi Nguyen, Duyen Thi Cam Nguye and Thuan Van Tran (2022) ‘Formation, antimicrobial activity, and biomedical performance of plant-based nanoparticles’ Environmental Chemistry 20:2531–2571.

Rahman S., Rahman L. Khalil A.T., Ali N., Zia D., Ali M., Shinwari Z. K (2019) ’Endophyte-mediated synthesis of silver nanoparticles and their biological applications’, Applied Microbiology and Biotechnology 103, 2551–2569.

Ramesh P. & Rajendran A., (2023) ‘Green synthesis of manganese dioxide nanoparticles: photocatalytic and antimicrobial investigations’ Int. J. Environ. Anal. Chem. doi.org/10.1080/03067319.

Salam HA, Rajiv P, Kamaraj M, Jagadeeswaran P, Gunalan S, Sivaraj R.(2012) ‘Plants: Green route for nanoparticle synthesis’ I Res J Biological Sci 1:85-90.

Saod W. M., Hamid L.L., Alaallah N. J. , Ramizy A., (2022) ‘Biosynthesis and antibacterial activity of manganese oxide nanoparticles prepared by green tea extract’ Biotechnology Reports, 34, 1-7.

Saravanan, M.; Gopinath, V.; Chaurasia, M.K.; Syed, A.; Ameen, F.; Purushothaman, N. (2018) ‘Green synthesis of anisotropic zinc oxide nanoparticles with antibacterial and cytofriendly properties’ *Microb. Pathog*. **115**, 57–63.

Savi G. D., Bortoluzzi,A. J., & Scussel V. M. (2013) ‘Antifungal properties of Zinc-compounds against toxigenic fungi and mycotoxin’ *International Journal of Food Science and Technology, 48*(9), 1834–1840.

Shah R. K., Boruah F. and Parween N. (2015).’Synthesis and characterization of ZnO nanoparticles using leaf extract of Camellia sinesis and evaluation of their antimicrobial efficacy’. Inter. J. Current Microbio. and App. Sci., 4, 444.

Shanshool S. K., Shanan Z. J., (2023) ‘Green Synthesis of Manganese Dioxide Nanoparticles and its Biological’, Baghdad Science Journal,doi org/10.21123.8385.

Sharma N., Jandaik, S., & Kumar, S. (2016) ‘Synergistic activity of doped zinc oxide nanoparticles with antibiotics: Ciprofloxacin, ampicillin, fluconazole and amphotericin B against pathogenic microorganisms’ *Anais Da Academia Brasileira de Ciencias*, *88*(3), 1689-1698.

Sharma V.K, Yagard R.A, Lin Y. (2009) ‘Silver nanoparticles: Green synthesis and their antimicrobial activities’ Colloid and Interface Science, 145: 83-96.

Sileshi Dubale, Dereje Kebebe, Ahmed Zeynudin, Negera Abdissa, Sultan Suleman, Sonika Dawadi, Akash Gupta, Manita Khatri , Manganese dioxide nanoparticles: synthesis, application and challenges, Bull Mater Sci ,43:277.

Sujit Kumar Ghosh (2020) 'Diversity in the Family of Manganese Oxides at the Nanoscale: FromFundamentals to Applications' ACS Omega, vol .5, pp 25493−25504

Sun, Q., Li, J., & Le, T. (2018) 'Zinc Oxide Nanoparticle as a Novel Class of Antifungal Agents: Current Advances and Future Perspectives' *Journal of Agricultural and Food Chemistry*, *66*(43), 11209–11220.

Syed Ibrahim Shah • Zulfiqar • Tahirzeb Khan • Rajwali Khan • Sardar Ali Khan • Shaukat Ali Khattak •Gulzar Khan(2019) 'Study of structural, optical and dielectric properties of α-MnO2 nanotubes (NTS)' Journal of Materials Science: Materials in Electronics vol. 30:19199–19205.

Tabrez S., Musarrat J., Al-khedhairy A.A., (2016) 'Colloids and surfaces B: biointerfaces countering drug resistance, infectious diseases, and sepsis using metal and metal oxides nanoparticles: current status' Colloids Surf. Biointerfaces, 146, 70.

Ting Du , Siya Chen, Jinyu Zhang, Tingting Li, Ping Li, Jifeng Liu, Xinjun Du and Tirukoti Mounika, Shiddappa L. Belagali , K.T. Vadiraj (2023) 'Manganese oxide nanoparticles synthesis route, characterization and optical properties' Materials Today: Proceedings 75 ,72–76.

Vartika Srivastava · Mukarram Beg · Shivanjali Sharma · Abhay Kumar Choubey (2021) 'Application of manganese oxide nanoparticles synthesized via green route for improved performance of water-based drilling fluids' Applied Nanoscience 11, 2247–2260.

Vijayamari A. A., Sadayandi K. S., Suresh S.S., Singh P. S.,(2017) 'A study of optical, surface morphological and electrical properties of manganese oxide nanoparticles' J Mater Sci: Mater Electron 28:2739–2746.

Vineet Kumar, Kulvinder Singh (2017) 'Green synthesis of manganese oxide nanoparticles for the electrochemical sensing of p-nitrophenol'Int Nano Lett, Vol 10.1007.

Wang S. (2020) ‘Antibacterial Activity of ManganeseDioxide Nanosheets by ROS-Mediated Pathways and Destroying Membrane Integrity nanomaterials’ . vol 10, 1545.

Xiaoxia Cai, Qingxia Zhu, Yun Zeng, Qi Zeng, Xueli Chen, Yonghua Zhan(2019) ‘Manganese Oxide Nanoparticles As MRI Contrast Agents In Tumor Multimodal Imaging And Therapy, International Journal of Nanomedicine’ International Journal of Nanomedicine, 14, 8321–8344.

Yudong Sun, Yifei Wang, Yaqi Liu, Huimin Wang, Changying Yang, Xiaoqing Liu and Fuan Wang (2022) ‘Integration of Manganese Dioxide-Based Nanomaterials for Biomedical Applications’ Advanced NanoBiomed Research doi.org/10.1002.

Zuzanna Sobanska, Joanna Roszak, Kornelia Kowalczyk and Maciej Stepnik(2021) ‘Applications and Biological Activity of Nanoparticles of Manganese and Manganese Oxides in In Vitro and In Vivo Models’, nanomaterials,11, 1084.